A dissertation submitted for the doctoral degree of science

Water diffusion in silica glass toward understanding of atomistic diffusion mechanism in silicate melts and glasses

(石英ガラス中の水の拡散：
ケイ酸塩メルトおよびガラス中における拡散メカニズムの原子スケールでの理解に向けて)

Presented by Minami Kuroda

Department of Natural History Sciences
Graduate School of Science
Hokkaido University

March, 2019

Abstract

Water diffusion in silicate melts is a fundamental process controlling physical and chemical consequences of magmatism, but mechanism of diffusion in silicate glasses and melts are not fully understood yet. In this study, with the aim of improving our understanding of the mechanisms of water diffusion in silicate melts and glasses including hydrogen isotope effects, I performed water diffusion experiments of water in silica glass and discussed the diffusion mechanism of water in silicate melt and glasses. The thesis consists of three parts as follows:

(1) Effect of structural dynamical property of melt on water diffusion in rhyolite melt:

Diffusion coefficients of water in rhyolite melt reported in previous studies are discussed in the context of water diffusion model in silica glass. The model well explains the water concentration dependence of water diffusivity in rhyolite melt, considering the effect of water concentration on activation energy of diffusion. The water concentration dependence of activation energy can be explained by the change of structural dynamical property of melt (i.e., viscosity), and the empirical relation between the water diffusivity and viscosity is also explained by the present model. Therefore I conclude that the water diffusion model proposed for silica glass (Kuroda et

al.. 2018) can be applied to rhyolite melt and that the water diffusion in rhyolite melt is controlled by the same atomic process as in silica glass.

(2) Hydrogen isotopic exchange in hydrated silica glass:

Hydrogen isotopes can be a useful tracer of magmatism and eruption. I performed hydrogen isotope exchange experiments between water vapor and hydroxyls in silica glass for fundamental understanding of the hydrogen isotope fractionation between silicate glasses and water vapor. Obtained hydrogen isotope exchange profiles show that the surface isotope exchange reaction and diffusion of hydrogen isotopes, which are carried as molecular water, occur simultaneously. I also found that the surface exchange reaction between $^{1}H_2O$ and ^{2}H in glass proceeds 1.7 times faster than that between $^{2}H_2O$ and ^{1}H in glass, which is a dominant cause of isotope fractionation profiles inside the glasses. The large difference of surface isotope exchange rate implies that a reaction involving hydrogen atoms controls the isotope exchange at the glass surface. The large kinetic isotope fractionation of hydrogen between water vapor and hydroxyls in glass may occur in a time scale of a few hours, and could affect the hydrogen isotope fractionation between dissolved water in magma and degassed water (i.e., bubbles) in an ascending magma.

(3) Fast diffusion path for water in silica glass:

Diffusion experiments of ^2H_2O at 900-750°C and water vapor pressure of 50 bar found more than one-order of magnitude faster diffusion of water in SiO_2 glass than that reported previously. The fast diffusion profile of water was observed as an extended tail of the normal water diffusion profile by a line scan analysis with SIMS, and it can be fitted with a diffusion model with a constant diffusivity. The obtained fast diffusion coefficient suggests that the diffusion species responsible for the fast diffusion is not molecular hydrogen but molecular water. The diffusivity and activation energy for the fast water diffusion can be explained by the correlation between diffusivities of noble gases in silica glass and their sizes. Because noble gases diffuse through free volume in the glass structure, we conclude that molecular water can also diffuse through the free volume. The abundance of free volume in the silica glass structure estimated previously is higher than that of ^2H observed in the fast diffusion in this study, suggesting that the free volume were not fully occupied by ^2H under the present experimental condition. This implies that the contribution of the fast water diffusion to the total water transport in volcanic glass becomes larger under higher water vapor pressure conditions.

These new findings improve our understanding of the mechanism of water diffusion in silicate melts/glasses, and would make a contribution to better understanding of volcanic activities.

Contents

Chapter 1

General introduction

Diffusion occurs through a thermal activated atomic-scale random motion of atoms, ions and molecules in minerals, glasses, and melts. This diffusion process is recorded as heterogeneous spatial distributions (zoning structure) of chemical or isotopic composition in minerals or glasses. Petrologists and geochemists often use this chemical or isotopic zoning to solve many problems, for instance, estimation of the formation conditions of minerals (e.g., Oeser et al., 2015) and thermal history of rocks (e.g., Takahashi, 1980; Sio et al., 2013). Diffusion data are also used to discuss bubble size distribution in volcanic rocks (e.g., Toramaru, 1989; Cross et al., 2012; Martel and Marziano, 2014), and processes influencing volcanic eruptions (e.g., Massol and Koyaguchi, 2005; Lloyd et al., 2014). Diffusion in minerals and melts affects on microscopic processes (e.g., formation of minerals and bubbles) and further has influence on macroscopic geologic events (e.g., changing an eruption style). Hence, it is important to obtain diffusion data and construct proper diffusion models from laboratory experiments for understanding geological events from microscopic to macroscopic view. In particular, understanding of diffusion mechanism is essential to apply the diffusion data obtained under limited conditions in laboratory to diffusion process under various physical and chemical conditions in nature.

Water diffusion in silicate melts and glasses is important especially in a field of volcanology. Water is the most abundant volatile component in magma, and its diffusion in magma strongly affects volcanic activity, for example, bubble nucleation and bubble growth rate in magma. Oversaturation of dissolved water in magma leads to bubble nucleation and growth by diffusion, providing the driving force of eruption (e.g.,

Zhang et al., 2007). The bubble growth rate affects the magma ascent rate and could be the main parameter controlling the eruption style. Many studies therefor have used water diffusion data to estimate magma ascent rates from natural samples based on water concentration profiles in volcanic glasses or bubble size distributions in volcanic rocks and to compare the estimated ascent rates with observed eruption styles in order to understand the critical factor governing the volcanic eruption style (e.g., Liu et al., 2007; Lloyd et al., 2014). It is thus critically important in the field of volcanology to fully understand water diffusion in silicate melts in a wide range of water concentration and melt composition to discuss water diffusion data under various magmatic conditions.

Because of its importance, water diffusion in silicate melts and glasses, as a potential analog of silicate melts, have been so far studied intensively (e.g., Doremus, 1969; 1995; 2000; Wakabayashi and Tomozawa, 1989; Tomozawa et al., 1994; Zhang and Behrens, 2000; Behrens, 2010; Kuroda et al., 2018; 2019). Water dissolves into silicate melts and glasses as two species; one is molecular water (referred as H_2O_m) and the other is hydroxyl (referred as OH) (e.g., Stolper, 1982). H_2O_m and OH can interconvert in silicate melts and glasses through the following reaction (e.g., Stolper, 1982):

$$H_2O_m + O \leftrightarrow 2OH \qquad (1\text{-}1)$$

where O represents anhydrous oxygen in silicate melts or glass structure. Both H_2O_m

and OH can be detected independently by IR spectroscopy (e.g., Zhang, 1999; Mcintosh et al., 2017) or Raman spectroscopy (e.g., Losq et al., 2013; Ni et al., 2013), and the equilibrium constant (K) of the reaction (1-1) is defined as:

$$K = \frac{{X_{OH}}^2}{X_{H_2O_m} X_O} \quad (1\text{-}2)$$

where X_i represents a mole fraction of a single oxygen atom in the species i. The total water concentration (X_{H2Ot}) is given by the sum of the concentration of the two water species:

$$X_{H_2O_t} = X_{H_2O_m} + \frac{X_{OH}}{2}. \quad (1\text{-}3)$$

The X_{H2Om} and X_{OH} have different dependence on X_{H2Ot} and hydroxyl is the dominant species at the low water concentrations, while molecular water becomes dominant at high water concentrations (e.g., Zhang and Ni, 2010). The time required for the reaction (1-1) to reach equilibrium is considered to be less than a second for silicate glass and melts at high temperatures (e.g., >~650°C for silica glass) (Doremus, 1999; Zhang and Ni, 2010).

In general, the main diffusion species for the water diffusion in silicate melts and glasses is considered to be molecular water. Zhang et al. (1991) performed dehydration diffusion experiments for rhyolite glass with ≦1.7 wt% of H_2O_t at

403-550°C and 1 bar of total pressure, and measured the water diffusion profiles with FTIR. By considering the inter-conversion reaction between H_2O_m and OH (reaction (1-1)), they concluded that OH diffusivity is about six orders of magnitude smaller than that of H_2O_m in Si-rich silicate melts and glasses. On the other hand, the OH diffusivity may not be negligibly small in Si-poor silicate melts (andesite and basalt melts) at high temperatures and low water contents (OH diffusivity is about one order of magnitude smaller than that of H_2O_m) (Ni et al., 2013; Zhang et al., 2017).

Another characteristic feature of water diffusion in silicate melts and glasses is its dependence on the water concentration. Doremus (1969, 1995) reported that water diffusivity in silica glass depends on the water concentration linearly at 650-1000°C based on published data. This dependence is consistent with that reported by Behrens (2010) for silica glass at 521-1097°C at 2 kbar. However, the concentration independent diffusion of water was also observed for silica glass at low water pressure (0.5 bar) and low temperature (400-600°C) by Wakabayashi and Tomozawa (1989). Regarding silicate glasses and melts, Doremus (2000) showed linear concentration dependence of water diffusion in rhyolite melts at 650-1000°C and a water pressure of 0.7-5 kbar with literature data. Zhang and Behrens (2000) showed the empirical relation of water diffusivity to the water concentration in rhyolite glasses and melts over a wide range of both temperature and pressure (400-1200°C and 0.01-8.1 kbar).

Kuroda et al. (2018) performed water diffusion experiments for silica glass at 650-850°C and discussed its diffusion mechanism with the aim of constructing a general water diffusion model in silica and silicate glasses, which can explain various

water concentration dependence of water diffusivity observed in previous studies. They proposed a new water diffusion model for silica glasses, where molecular water diffuse through diffusion pathways formed by breaking Si-O-Si bond through hydroxyl formation reaction (Eq. (1-1)). Their model explains the stronger water concentration dependence of water diffusion in silica glass at low water concentrations than that in silicate glasses, and also explains both linear and no water concentration dependence reported for silica glass (Doremus, 1969, 1995; Behrens, 2010; Wakabayashi and Tomozawa, 1989). They proposed that their water diffusion model in silica glass could be applicable to water diffusion behavior in silicate glasses (for instance, exponential water concentration dependence of water diffusivity in rhyolite melt: Zhang and Behrens, 2000). However, detailed discussion on the concentration dependence of water diffusion in silicate melts and glasses and the mechanisms by which water diffuses through silicate melts and glass structures has not been fully made yet.

The degassing process of magma could also be deduced from hydrogen isotopic composition (δD) and water concentration in volcanic glasses (e.g., Taylor et al., 1983; Nakamura et al., 2008 and references therein; Castro et al., 2014). The degree of hydrogen isotopic fractionation (δD) is correlated with the water concentration in natural volcanic samples: δD decreases with decreasing the water concentration and the degree of decrease in δD is more pronounced at the lower water concentration. This trend has been interpreted to reflect the transition of water degassing style from a closed-system batch degassing to an open-system Rayleigh degassing. An elementary process that has often been neglected to discuss the relation between δD and water

concentration in the previous studies is the fractionation during diffusive transport of water in magma (i.e., kinetic isotope fractionation invloving hydrogen isotope exchange reaction and diffusion). Detailed understanding of hydrogen isotope fractionation process between silicate melts/glasses and water vapor/fluid is needed to elucidate the degassing processes from hydrogen isotopes.

There have been only a few studies for the hydrogen isotope fractionation during water diffusion. Lapham et al. (1984) investigated the difference of diffusivities of $^{1}H_2O$ and $^{2}H_2O$ in rhyolite melt. Their data showed that the diffusivity of $^{1}H_2O$ is twice as large as that of $^{2}H_2O$ in rhyolite melt. However, a more recent study (Anovitz et al., 2008) reported that there is no measurable difference between the diffusivities of $^{1}H_2O$ and $^{2}H_2O$ in rhyolite glass. Anovitz et al. (2009) further performed hydrogen isotope exchange reaction experiments between water vapor and hydrated rhyolite glass at 148°C. They found that hydrogen isotope exchange reaction occurs even at low temperature, but no detail discussion (e.g., the isotope exchange reaction rate and its dependence on temperature, glass composition, and pressure) has been made.

In this study, with the aim of improving our understanding of the mechanism of water diffusion in silicate melts and glasses including isotope effects, I performed diffusion experiments of water in silica glass and discussed the diffusion mechanism of water in silicate melt and glasses. In chapter 2, I apply the water diffusion model proposed by Kuroda et al. (2018) to water diffusion in rhyolite melt and to discuss the effect of silicate melt structure on water diffusion. In chapter 3, to understand the kinetic hydrogen isotope fractionation between water vapor and hydroxyls in silica glass,

I performed hydrogen isotope exchange experiments between hydrated silica glass and water vapor and found that a large hydrogen isotope fractionation could occur due to the kinetic isotope exchange reaction at the glass surface, which can be a cause of large hydrogen isotope fractionation between volcanic glass and water vapor. In chapter 4, a new fast diffusion pathway for water in silica glass was found by the diffusion experiments using $^{2}H_2O$ (^{2}H was used as a tracer of water), through which water can be transported at a rate of one-order of magnitude faster than previously reported (Kuroda et al., 2018). In chapter 5, I summarize all the findings in this theses including future works.

Chapter 2

Effect of structural dynamical property of melt on water diffusion in rhyolite melt

2-1. Introduction

Water in silicate melts plays an important role to control both chemical and physical properties of the melt. Dissolved water decreases melt viscosity, and promotes mineral crystallization and bubble growth in ascending magmas (e.g., Tomozawa et al., 1994; Zhang et al., 2007), which changes the volcanic eruption style. Diffusion of water in silicate melts is one of the essential controlling factors of bubble nucleation and growth in magma.

Water diffusion in various silicate melts and glasses, as an analog of silicate melts, have been intensively studied because of its importance in volcanology (e.g., Doremus, 1969; Nowak and Behrens, 1997; Doreums, 2000; Zhang et al., 2007; Persikov et al., 2014; Ni et al., 2015). Although it is widely known that water diffusivity depends on water concentration and melt composition, its fundamental atomistic mechanism in a wide range of melt composition and water concentration has not yet been fully understood.

Kuroda et al. (2018) performed water diffusion experiments in silica glass to understand a fundamental mechanism of water diffusion in interconnected SiO_4 tetrahedra. They found that water diffusion in silica glass has stronger water-concentration dependence than that in silicate glasses, which was explained by diffusion of molecular water (H_2O_m) through diffusion pathways formed by hydroxyls (-OH). In this study, this water diffusion model in silica glass is applied to water diffusion in rhyolite melts, of which water diffusion has been well studied, to understand an atomic-scale process of water diffusion in silicate melts.

2-2. Application of water diffusion model in silica glass to rhyolite melt

The water concentration dependence of water diffusion in silica glass can be attributed to a limited number of diffusion pathways formed through hydroxyl formation reaction ($H_2O_m + O \leftrightarrow 2OH$) (Fig. 2-1) (Kuroda et al., 2018). The model is applied to multi-component silicate melts by taking the effects of metal cations into account, which also provide diffusion pathways by forming non-bridging oxygen (NBO). In this case, the diffusivity of total water ($D_{H_2O_t}$) can be given as:

$$D_{H_2O_t} = D_{H_2O_m}\frac{\partial X_{H_2O_m}}{\partial X_{H_2O_t}}$$

$$= [Jump\ frequency\ of\ H_2O_m][Jump\ distance]^2[Number\ of\ diffusion\ pathways]\frac{\partial X_{H_2O_m}}{\partial X_{H_2O_t}}$$

$$= \nu\lambda^2 exp\left(-\frac{E_a}{RT}\right)\left(\frac{X_{OH}}{2} + kX_{NBO}\right)\frac{\partial X_{H_2O_m}}{\partial X_{H_2O_t}}$$

$$= D^*\left[kX_{NBO} + \frac{K}{4}\left(\left(1 + \frac{16X_{H_2O}}{K}\right)^{1/2} - 1\right)\right]\left[1 - \left(1 + \frac{16X_{H_2O}}{K}\right)^{-1/2}\right], \qquad (2\text{-}1)$$

where D_i and X_i represent the diffusion coefficient and the mole fraction of a single oxygen atom in the species *i*, ν is the molecular vibration frequency, λ is the jump distance, E_a is the activation energy for diffusion, R is the gas constant, T is absolute temperature, K is the equilibrium constant of hydroxyl formation reaction (Zhang and NI, 2010), and k is a parameter to relate X_{NBO} to the number of diffusion pathways ($0 \leq k \leq 1$) (Kuroda et al., 2018). When all monovalent and divalent metal cations act as network-modifier cations and all non-bridging oxygen atom generate one diffusion

pathways, k is equal to unity. Eq. (2-1) is equivalent to the water diffusivity in silica glass when X_{NBO} =0 (Kuroda et al., 2018).

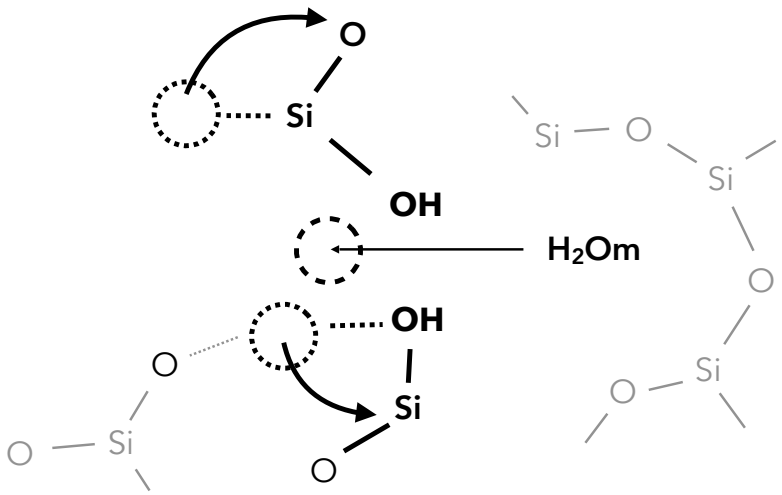

Figure 2-1.

A schematic illustration of diffusion of molecular water in silicate melts. A water molecule diffuses through a pathway formed by hydroxyls or network modifier cations. When diffusivities of Si and O are enhanced by dissolved water, the network rearrangement due to their diffusion could lower the energy barrier for molecular jump.

I found that Eq. (2-1) explains the water concentration dependence of water diffusion coefficients reported for rhyolite melt (Nowak and Behrens, 1997) irrespective of k only at low water concentration (dotted curves in Fig. 2-2). However, the model

cannot explain the water diffusivity in a wide range of water concentration, showing a concave upward relation to water concentration, where water diffusion is more promoted than that predicted in the model.

The activation energy (E_a) for water diffusion in rhyolite melt is known to decrease with increasing the water content (0.5–6 wt%; Fig. 2-3) (Nowak and Behrens, 1997). This dependence was attributed to the change of melt viscosity with water concentration (Nowak and Behrens, 1997), but no detailed discussion has been made yet. In this study, the relation between the water concentration and the decrease of E_a in Nowak and Behrens (1997) was fitted as a logarithm function (Fig. 2-3):

$$\Delta E_{a,wat}\ (kJ/mol) = -8.61\ ln\left(\frac{X_{H_2O_t}}{X_{0.9}}\right), \quad (2\text{-}2)$$

where $\Delta E_{a,wat}$ is the change of E_a from that at the H_2O concentration of 0.9 mol% ($X_{0.9}$) (0.5 wt%) in the melt. This empirical expression diverges to positive infinity when $X_{H_2O_t}$ approaches to zero, but $\Delta E_{a,wat}$ ranges from 0 to -18 kJ/mol within the range of $X_{H_2O_t}$ discussed in this study (0.5–6 wt%).

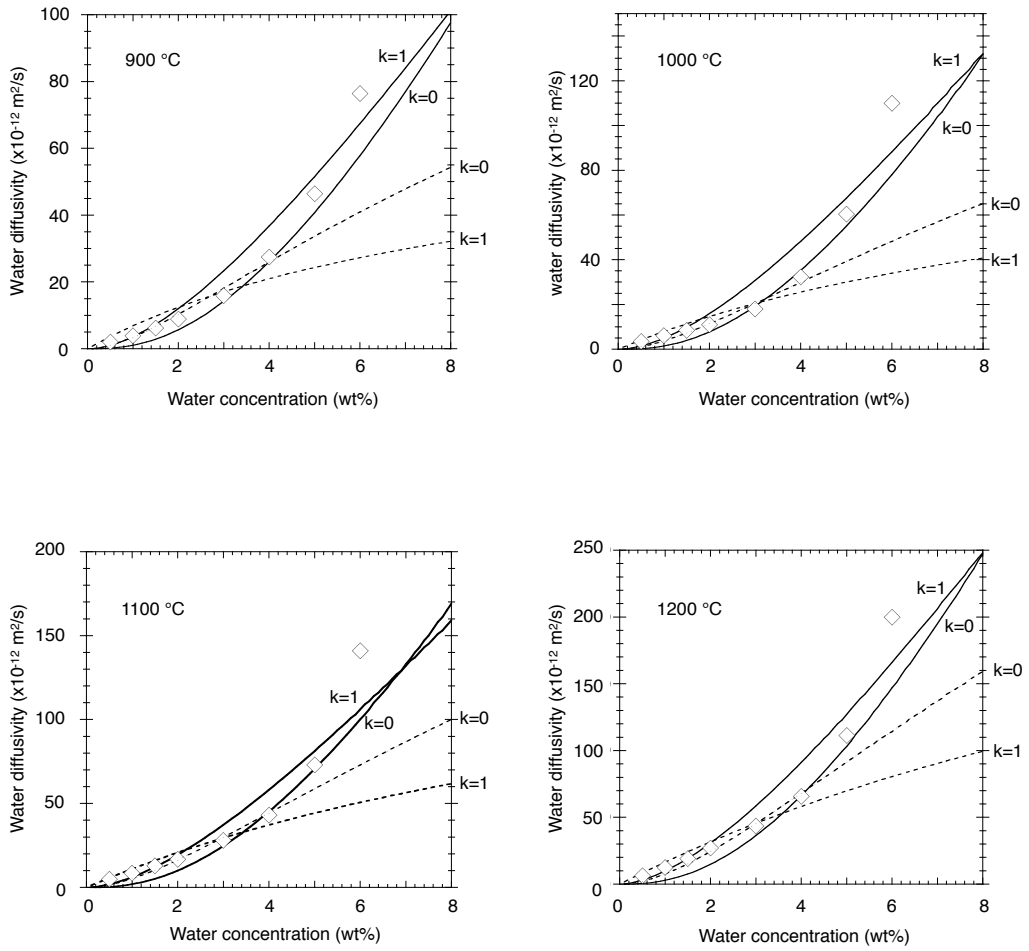

Figure 2-2.

Water concentration dependence of diffusivity for rhyolite melt (Nowak and Behrens, 1997). The water diffusivity data are fitted with the water diffusion model proposed in this study: dashed curves (Eq. (2-1) with k=1 and 0) and solid curves (Eq. (2-4) with k=1 and 0). The fitting with Eq. (2-1) was made only for the diffusivity data with water concentration smaller than 4 wt% to show the deviation of the model from the data at higher water concentrations. The model including the decrease of E_a with increasing water concentration well explains the data.

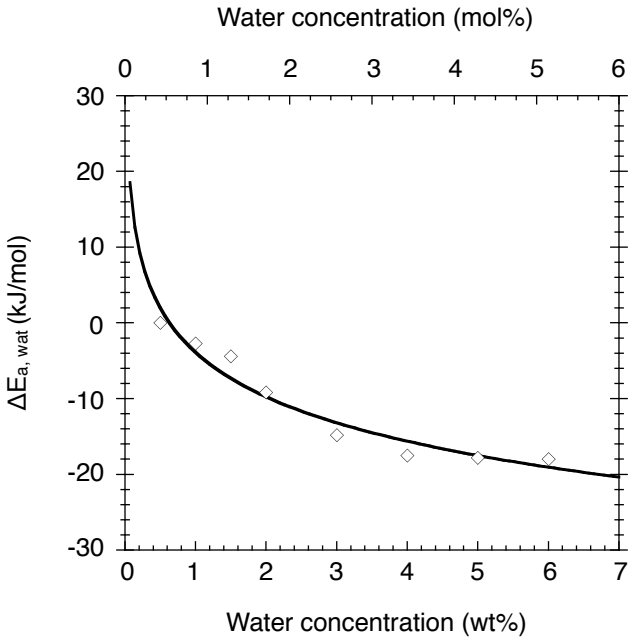

Figure 2-3.

The relation between the activation energy for water diffusion and water concentration in rhyolite melt (data from Nowak and Behrens, 1997). The activation energy is shown as a relative difference from that at the total water concentration of 0.5 wt% ($\Delta E_{a,\,wat}$).

The effect of water concentration on E_a (Eq. (2-2)) is included in Eq. (2-1) as follows:

$$D_{H_2O_t} = \nu\lambda^2 exp\left(-\frac{E_a+\Delta E_{a,wat}}{RT}\right)\left(\frac{X_{OH}}{2} + kX_{NBO}\right)\frac{\partial X_{H_2O_m}}{\partial X_{H_2O_t}}. \quad (2\text{-}3)$$

By combining all the concentration-independent terms into D^*, the diffusion coefficient of total water can be given by:

$$D_{H_2O_t} = D^* exp\left(-\frac{\Delta E_{a,wat}}{RT}\right)\left(\frac{X_{OH}}{2} + kX_{NBO}\right)\frac{\partial X_{H_2O_m}}{\partial X_{H_2O_t}}$$

$$= D^* exp\left(-\frac{\Delta E_{a,wat}}{RT}\right)\left[kX_{NBO} + \frac{K}{4}\left(\left(1 + \frac{16X_{H_2O_t}}{K}\right)^{1/2} - 1\right)\right]\left[1 - \left(1 + \frac{16X_{H_2O_t}}{K}\right)^{-1/2}\right] \quad (2\text{-}4)$$

The water diffusivity in rhyolite melts (Nowak and Bherens, 1997) are fitted with Eq. (2-4) for k=1 or 0 (Fig. 2-2). Eq. (2-4) fits the water diffusivity in rhyolite melt better than Eq. (2-1) in a wide range of water concentration. The chemical composition of rhyolite melt in Nowak and Behrens (1997) suggests NBO/T of ~0 for the melt, implying that monovalent and divalent cations in rhyolite melt in Nowak and Behrens (1997) do not act as network modifiers due to the presence of Al^{3+} in the network of tetrahedra (k=0). However, the present model cannot quantitatively determine k for the melt.

2-3. Discussion

The model for water diffusion in silica glass (Kuroda et al., 2018) can explain the water diffusion in rhyolite melt with taking the decrease of E_a with water concentration into account. Here I attribute the change of E_a to the effect of structural dynamical property of melt on water diffusion. Viscosity is a bulk property of melt, and

has been measured for various silicate melts including the effect of dissolved water. Viscosity is microscopically related to diffusivities of Si and O atoms, which construct the network structure of silicate melts, by the Eyring relation (Ni et al., 2015; Eyring, 1936). In low-viscosity silicate melts, the diffusive movement of Si and O in the melt structure may lower the activation energy of molecular jump and enhance the water diffusivity through network rearrangement (Fig. 2-1).

Here I consider that the empirical relation of $\Delta E_{a,wat}$ with dissolved water concentration (Eq. (2-2)) is caused by decrease of viscosity (η) due to increase of water concentration. In order to include the viscosity effect into the model, the relation of $\Delta E_{a,wat}$ and water concentration (Nowak and Behrens, 1997) (Eq. (2-2)) was converted into the relation between $\Delta E_{a,wat}$ and η as follows; (1) Based on the relation between viscosity, water concentration, and temperature (Zhang et al., 2003), the relationship between $\Delta E_{a,wat}$ and water concentration (0.1–8 wt%) (Fig. 2-3; Eq. (2-2)) was changed to that between $\Delta E_{a,wat}$ and η at different temperatures (Fig. 2-4). (2) $\Delta E_{a,wat}$ and ln η show a liner relation at each temperature, and d($\Delta E_{a,wat}$)/d(ln η) of 2.55, 2.86, 3.19, and 3.53 are obtained at 900, 1000, 1100, and 1200°C, respectively. (3) Using the average d($\Delta E_{a,wat}$)/d(ln η) at different temperatures (A = 3.03), the relationship between $\Delta E_{a,vis}$ and η is given by:

$$\Delta E_{a,vis}\ (kJ/mol) = A\ ln\left(\frac{\eta}{\eta_0}\right) \tag{2-5}$$

where $\Delta E_{a,vis}$ is the relative difference of E_a from that at the viscosity at the glass transition temperature (η_0 = 10^{12} Pa s). The choice of the reference viscosity (η_0) does not affect the discussion below.

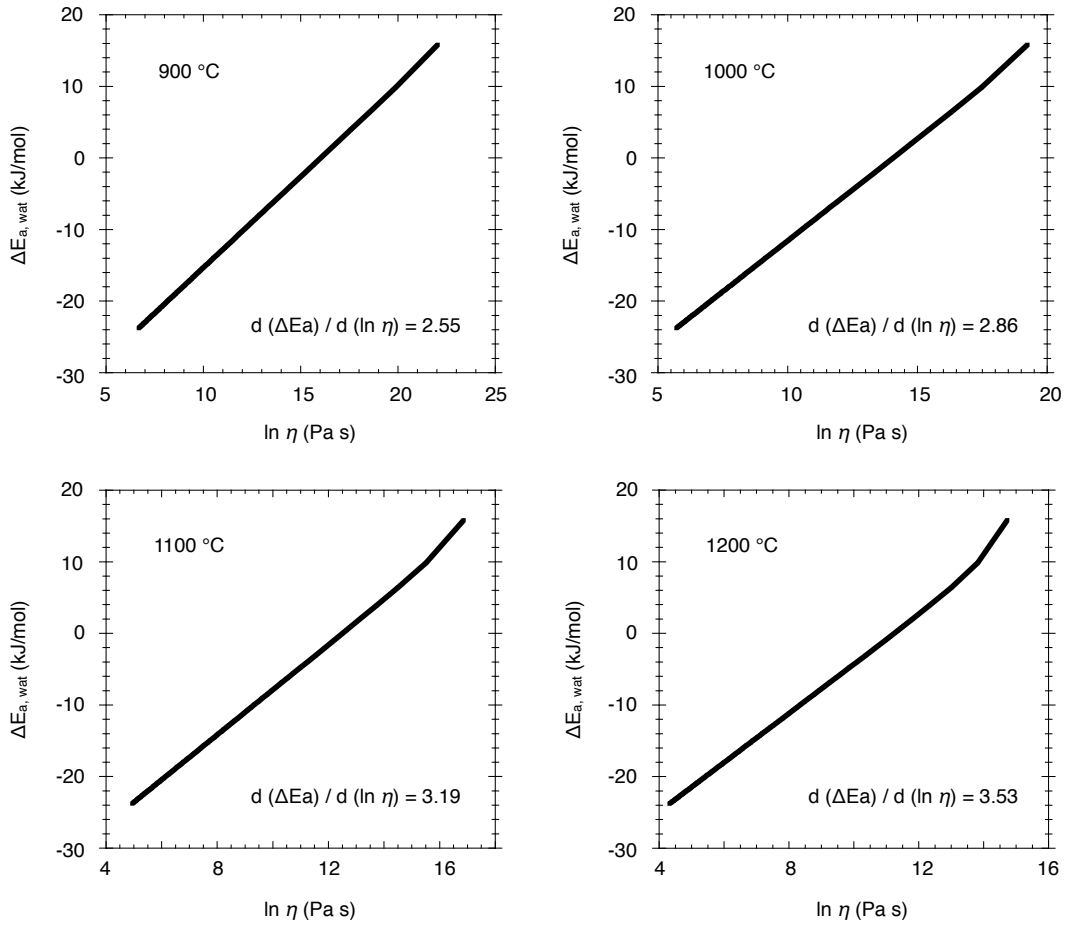

Figure 2-4.

The relation between $\Delta E_{a,\,wat}$ and melt viscosity of rhyolite melt at 900, 1000, 1100, and 1200 °C (see details in the text).

The water diffusivity is expressed as follows using Eq. (2-5):

$$D_{H_2O_t} = \nu d^2 exp\left(-\frac{E_a+\left[Aln\left(\frac{\eta}{\eta_0}\right)\right]}{RT}\right)\left(\frac{X_{OH}}{2}+kX_{NBO}\right)\frac{\partial X_{H_2O_m}}{\partial X_{H_2O_t}}$$
$$= \nu d^2 \left(\frac{\eta}{\eta_0}\right)^{-\frac{A}{RT}} exp\left(-\frac{E_a}{RT}\right)\left(\frac{X_{OH}}{2}+kX_{NBO}\right)\frac{\eth X_{H_2O_m}}{\partial X_{H_2O_t}} \quad (2\text{-}6)$$

By combining all water concentration- or melt composition-independent terms into *D*, the diffusion coefficient of total water can be given as;

$$D_{H_2O_t} = D\left(\frac{\eta}{\eta_0}\right)^{-\frac{A}{RT}}\left(\frac{X_{OH}}{2}+kX_{NBO}\right)\frac{\partial X_{H_2O_m}}{\partial X_{H_2O_t}}. \quad (2\text{-}7)$$

The water diffusivity in silicate melts depends on viscosity in the form of $\left(\frac{\eta}{\eta_0}\right)^{-\frac{A}{RT}}$. The viscosity dependence of water diffusion in various silicate melts has been empirically known to be proportional to $\eta^{-0.269}$ for silicate melt with $\eta > 10^{2.5}$ Pa s (Persikov et al., 2010). The multiplier of η in Eq. (2-7) (*A/RT*) ranges from 0.26 to 0.29 in the temperature range considered here, and is well consistent with the empirical relation between the water diffusivity and melt viscosity. Because the term $\left(\frac{X_{OH}}{2}+kX_{NBO}\right)\frac{\partial X_{H_2O_m}}{\partial X_{H_2O_t}}$ in Eq. (2-7) does not change significantly with η, the water diffusion model in this study can explain the empirical dependence of water diffusivity on the melt viscosity.

Kuroda et al. (2019) found fast diffusion pathways for H_2O molecules in

silica glass at 900-750°C with water vapor pressure of 50 bar. A small fraction of dissolved water molecules diffuse through connected free volume (not through the pathways formed by OH), and the activation energy for diffusion is explained by

$$E_a = 8\pi G r_0 (r - r_0)^2, \quad (2\text{-}8)$$

where G represents a shear modulus of the silica glass (30 GPa for silica glass (Znderson and Stuart, 1954)), r and r_0 are radii of the diffusion species and the diffusion gateway, respectively (Anderson and Stuart, 1954; Zhang and Xu, 1995). Because the fast diffusion of H_2O molecules in silica glass occurs within the pre-existing network structure, its activation energy is likely to simply represent the energy required for molecular jump.

The shear modulus of silicate melts (G) is negatively proportional to temperature (Bansal and Doremus, 1986; Schilling et al., 2003; Falenty and Webb, 2010). The temperature dependence of G is in order of -0.01 GPa/K, and its change with temperature cannot be recognized in diffusion experiments. On the other hand, the viscosity of silicate melts (η) has larger temperature dependence than G. The temperature dependence of η is modeled by the VFT equation (Vogel, 1921; Hess and Dingwell, 1996), but in the temperature range considered here, it can be approximated to the Arrhenius elation ($\eta = A \exp(B/T)$). Assuming that the temperature dependence of G is caused by the change of viscosity with temperature, the temperature dependence of G can be converted into its viscosity dependence as follows:

$$\Delta G \propto -\Delta T \propto -\left(ln\frac{\eta}{\eta_0}\right). \quad (2\text{-}9)$$

Therefore ΔE_a from the reference condition (η_0 of 10^{12} Pa s in this study) can be proportional to $\ln(\eta/\eta_0)$ as expressed by Eq. (2-5).

I thus conclude that the water diffusion model for silica glass (Kuroda et al., 2018) can explain water diffusion in rhyolite melts in wide ranges of temperature and water concentration by taking the change of activation energy of diffusion due to the change of structural dynamic property of melt (viscosity).

2-4. Conclusions

I applied the water diffusion model in silica glass (Kuroda et al., 2018) to water diffusion in rhyolite melt with considering decrease of the activation energy with water concentration. The new model explains the water concentration dependence of water diffusivity in rhyolite melt. The decrease of the activation energy with water concentration can be explained by the change of structural dynamic property of melt, where structural rearrangement due to enhanced diffusion of Si and O lowers the energy barrier for molecular jump in the melt with higher water concentration. The viscosity dependence of the diffusivity predicted by the model is also consistent with that observed empirically. These findings suggest that the diffusion of water in rhyolite melt

can be explained by the same atomic process as in silica glass.

Chapter 3

Hydrogen isotopic exchange in hydrated silica glass

3-1. Introduction

Water is the most abundant volatile component in magma. Water in silicate melts changes physical and chemical melt properties of the melts, and plays an important role to control magmatism and volcanic eruption in subduction zones, for instance, through lowering melting point of rocks and melt viscosities and increasing bubble nucleation and growth in magmas (Tomozawa et al., 1994; Zhang et al., 2007). Hydrogen isotope ration in volcanic glasses could provide useful information to track the interaction between dissolved water in magmas and water vapor in an open or closed system using an equilibrium isotopic fractionation factor (e.g., Nakamuta et al., 2006; Kyser and O'Neil, 1984; Taylor et al., 1983; Castro et al., 2014). However, hydrogen isotope exchange between magma/volcanic glass and water vapor/ fluid occurs in a short timescale or at low temperatures, where hydrogen isotope fractionation may need to discusses as a result of a series of time-dependent processes such as surface exchange reaction and diffusion, not as a simple fractionation in an open (Rayleigh) or closed (butch) system. Therefor, the fundamental understanding of elementary processes responsible hydrogen isotope exchange between magma/glass and water vapor/fluid is essential to interpret properly hydrogen isotope records in natural samples.

Lapham et al. (1984) firstly investigated the hydrogen isotope fractionation by water diffusion in rhyolite glass at 850°C with $^{1}H_2O$ or $^{2}H_2O$ vapor of 700 bar and reported that the diffusivity of $^{1}H_2O$ is twice as large as that of $^{2}H_2O$, which could cause a large diffusive D/H fractionation in the glass. On the other hand, Anovitz et al (2008,

2009) reported that there is no clear difference between diffusivity of $^{1}H_2O$ and $^{2}H_2O$ in rhyolite glass at 150°C. They also reported that the isotope exchange reaction between water vapor and dissolved water occurs even at low temperature (150°C) but no detail discussion was made about, for instance, temperature dependence, reaction mechanism and kinetic parameters of the isotope exchange reaction.

Here in order to understand elementary processes responsible for hydrogen isotope fractionation between silicate glasses/melts and water vapor/fluid, I performed two types of experiments at 50 bar of water vapor pressures; (1) $^{1}H_2O$ and $^{2}H_2O$ diffusion experiments in silica glass at 750°C, and (2) hydrogen isotope exchange experiments between $^{1}H_2O$ ($^{2}H_2O$) bearing silica glass and $^{2}H_2O$ ($^{1}H_2O$) vapor at 750-900°C.

3-2. Experimental and analytical methods

Diffusion experiments of $^{1}H_2O$ and $^{2}H_2O$ in silica glass were carried out at 50 bar of water vapor pressure and 750°C following the experimental protocol of Kuroda et al. (2018, 2019). An optical silica glass plate (5 mm × 3 mm × 2 mm) containing 10 ppm water and $^{1}H_2O$ or $^{2}H_2O$ water were enclosed in a glass tube (3.5 mm and 4.7 mm inner an outer diameter, and 80 mm length) and heated in a box furnace at 750°C for 20 hours (Table 1). The amount of water in the sealed glass tube was adjusted to make a 50 bar water vapor pressure at the experimental temperatures with complete evaporation.

Hydrogen isotope exchange experiments were performed at 750, 800, 850,

and 900°C with a similar experimental protocol using the same silica glass plate (5 mm × 3 mm × 2 mm) in the following way. The glass plate was enclosed with either $^{1}H_2O$ or $^{2}H_2O$ into a silica glass tube, and heated in the box furnace at 50 bar of water vapor pressure and a desired temperature for 20 hours (first-step heating). The glass plate was then taken out from the sealed glass tube, and re-sealed in a new silica glass tube with water enriched in the isotope counterpart ($^{2}H_2O$ for $^{1}H_2O$ an vice versa). The second-step diffusion was done at the same temperature as the first-step experiment for 1, 3, or 10 hours. All the experimental conditions are summarized in Table 1.

Concentration profiles of ^{1}H, ^{2}H, and ^{30}Si for a polished cross-section of the run products were measured with secondary ion mass spectroscopy (SIMS; CAMECA ims-6f) at Hokkaido University. A defocused primary beam of Cs+ of 10 keV was irradiated on the sample surface to make a flat crater with a diameter of 20-25 μm. The primary beam current was about 20 nA. Sputtered secondary ions were collected from the central region (10 μm in diameter) of the spattered area to minimize the ^{1}H signal from adsorbed water on the polished sample surface. A normal electrical flood was used for charge compensation. A few profiles (mostly three) were obtained for each sample to assess the analytical reproducibility by moving the sample stage with 5 μm steps across the sample surface.

Table 3-1. Summary of experimental conditions.

		1st heating		2nd heating	
T (°C)	P (bar)	vapor species	duration (h)	vapor species	duration (h)
750	50	$^{1}H_2O$	20	-	-
		$^{2}H_2O$	20	-	-
		$^{1}H_2O$	20	$^{2}H_2O$	1
		$^{2}H_2O$	20	$^{1}H_2O$	1
		$^{1}H_2O$	20	$^{2}H_2O$	3
		$^{2}H_2O$	20	$^{1}H_2O$	3
		$^{1}H_2O$	20	$^{2}H_2O$	10
		$^{2}H_2O$	20	$^{1}H_2O$	10
800	50	$^{1}H_2O$	20	$^{2}H_2O$	3
		$^{2}H_2O$	20	$^{1}H_2O$	3
850	50	$^{1}H_2O$	20	$^{2}H_2O$	3
		$^{2}H_2O$	20	$^{1}H_2O$	3
900	50	$^{1}H_2O$	20	$^{2}H_2O$	3
		$^{2}H_2O$	20	$^{1}H_2O$	3

3-3. Results

Typical diffusion profiles of ^{1}H or ^{2}H of the samples heated for diffusion experiments of $^{1}H_2O$ and $^{2}H_2O$ are shown with ^{30}Si and the isotope counterpart in Figures 3-1 ((a) and (b)). The typical profiles of both ^{1}H and ^{2}H for the isotopic exchange experiments are also shown with ^{30}Si in Figures 3-1 ((c) and (d)).

The concentration profiles of ^{1}H and ^{2}H in diffusion experiments of $^{1}H_2O$ and $^{2}H_2O$ show almost the same diffusion distances (Figures 3-1 (a) and (b)). This suggests that the diffusivities of $^{1}H_2O$ and $^{2}H_2O$ are not largely different as reported in Laphan et al (1984), but they are almost the same as observed by Anovitz et al (2008, 2009).

The ^{1}H and ^{2}H profiles in Figures 3-1 (c) and (d) show that ^{1}H or ^{2}H that diffused into the glass during the first step diffusion was exchanged with the isotope counterpart (^{2}H or ^{1}H) during the second step heating. The hydrogen isotope exchange profiles are obtained using the hydrogen isotope ratio (X_i) of

$$X_i = \frac{^{i}H}{^{1}H + ^{2}H} \tag{3-1}$$

where ^{i}H represents the hydrogen isotope used for the second-step heating (Figure 3-2).

The relative difference (R) between X_1 and X_2 inside the glasses heated under the same conditions is calculated as

$$R = \frac{1-X_2}{1-X_1}. \tag{3-2}$$

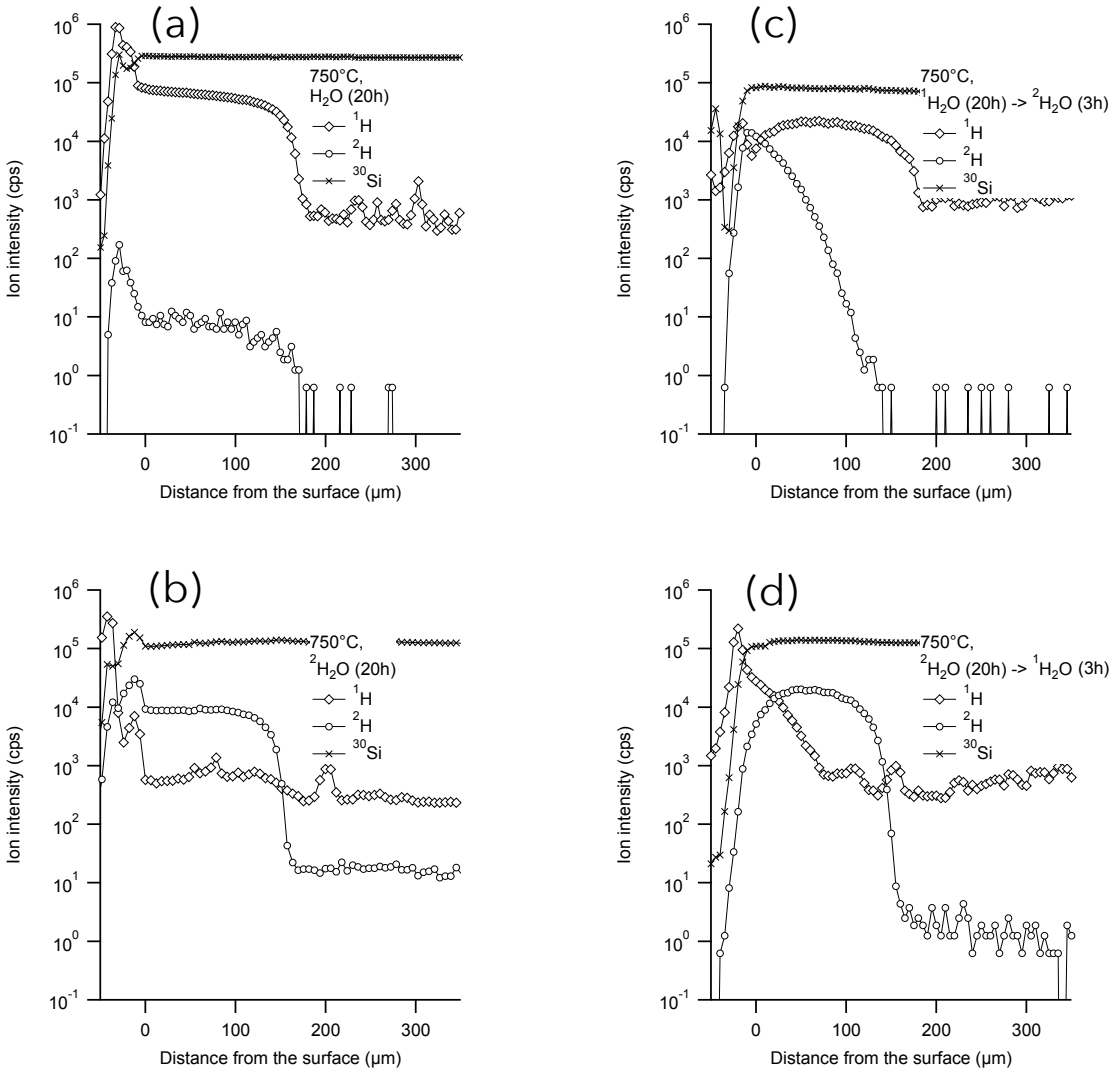

Figure 3-1. Typical ion intensity profiles of ^{1}H, ^{2}H, and ^{30}Si of the heated samples (a) 750°C, $^{1}H_2O$ of 50 bar for 20 hours. (b) 750°C, $^{2}H_2O$ of 50 bar for 20 hours. (c) 750°C, $^{1}H_2O$ of 50 bar for 20 hours followed by $^{2}H_2O$ of 50 bar for 3 hours. (d) 750°C, $^{2}H_2O$ of 50 bar for 20 hours hollowed by $^{1}H_2O$ of 50 bar for 3 hours. ^{1}H and ^{2}H signals inside the glass (deeper than -180 μm) are from backgrounds.

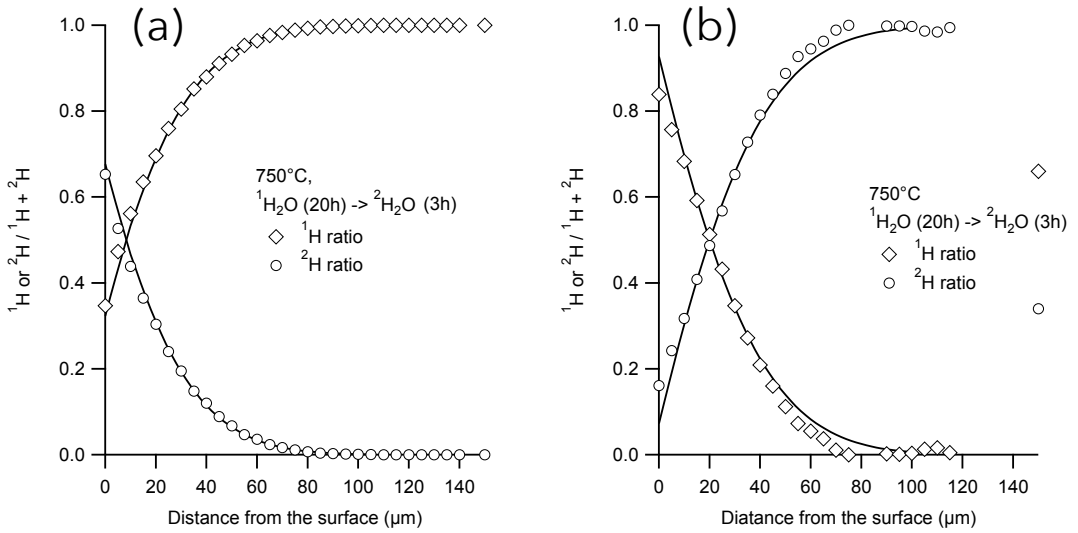

Figure 3-2. Typical hydrogen isotope exchange profiles inside glasses reacted with water vapor at 750°C. (a) ^2H_2O vapor and ^1H in silica glass. (b) ^1H_2O vapor and ^2H in silica glass. Isotope exchange profiles can be explained with Eq. (3-7) (solid curves).

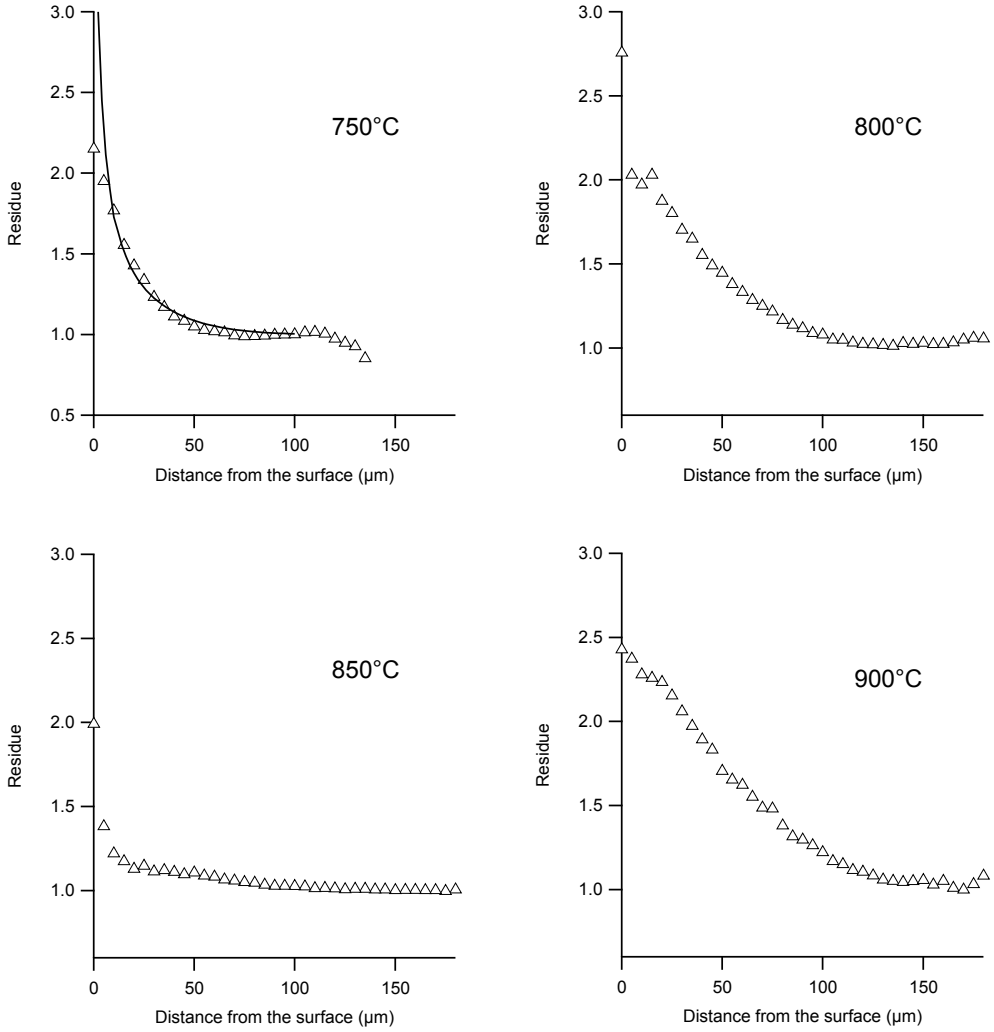

Figure 3-3. Typical residues obtain at 750, 800, 850, and 900°C. The profile of 750 °C can be explained with Eq. (3-7) (solid curves).

I used (1- X_i) instead of X_i in order to avoid dividing by 0 in the deep interior of glasses, where no water diffusion occurred (i.e., X_i=0). The R should be equal to unity where $X_1 = X_2$.

Typical profiles of R inside the glasses heated the different temperatures are shown in Figure 3-3. The R's in all the samples are larger than 0 and tend to decrease monotonically from the surface along concave profiles. This indicated that the isotope exchange between ^2H_2O vapor and ^1H in silica glass processed faster than that between ^1H_2O vapor and ^2H in silica glass.

3-4. Discussion

Here the cause of the difference of isotope exchange behaviors of ^2H_2O vapor with ^1H in silica glass and ^1H_2O vapor with ^2H in silica glass is discussed. I focus on the results obtained from the samples at 750°C.

3-4-1. Non-equilibrium hydrogen isotope exchange reaction at glass surface

The isotopic effect of the hydrogen isotope exchange rate at the glass surface could be the cause of isotope fractionation. The rate constants for the hydrogen isotope exchange reaction at the glass surface were estimated form the temporal change of the surface isotope compositions that were obtained from the concentration profiles measured with SIMS (Table 1).

The X_1 and X_2 at the glass surface ($X_{1,\,surface}$ and $X_{2,\,surface}$) increase with time (Figure 3-4), showing that the surface isotope compositions were not in equilibrium with water vapor during second-step heating, especially for samples with shorter heating durations. The $X_{1,\,surface}$ and $X_{2,\,surface}$ show different time-dependent trends, which may imply that the surface isotope exchange reaction is isotope-dependent.

The change of $X_{i,\,surface}$ can be expressed as

$$\frac{dX_{i,surface}}{dt} = k_i\left(1 - X_{i,surface}\right) \tag{3-3}$$

where k_i is the surface isotope exchange rate for $^{i}H_2O$ with H in the glass. Eq. (3-3) is integrated to be

$$X_{i,surface} = X_{i,\infty}(1 - e^{-k_i t}) \tag{3-4}$$

where $X_{i,\,\infty}$ is the isotope composition at t=∞, which should be determined by the equilibrium isotope fractionation factor between H_2O vapor and H in silica glass, and t is time during 2nd-step heating. In this study, $X_{1,\,\infty}$ and $X_{2,\,\infty}$ are given as 1 and 0.95 based on $X_{i,\,surface}$ of diffusion experiments of $^{1}H_2O$ and $^{2}H_2O$ (Figure 3-1 (a) and (b)). By fitting the data with Eq. (3-4), I obtained k_1 of 2.32 (±0.22) $\times 10^{-4}$ /s and k_2 of 1.39 (±0.11) $\times 10^{-4}$ /s (Figure 3-4), and found that k_1 is about 1.7 times larger than k_2 (k_1/k_2 = 1.67 ± 0.21). This difference of k_1 could be the cause of hydrogen isotope fractionation

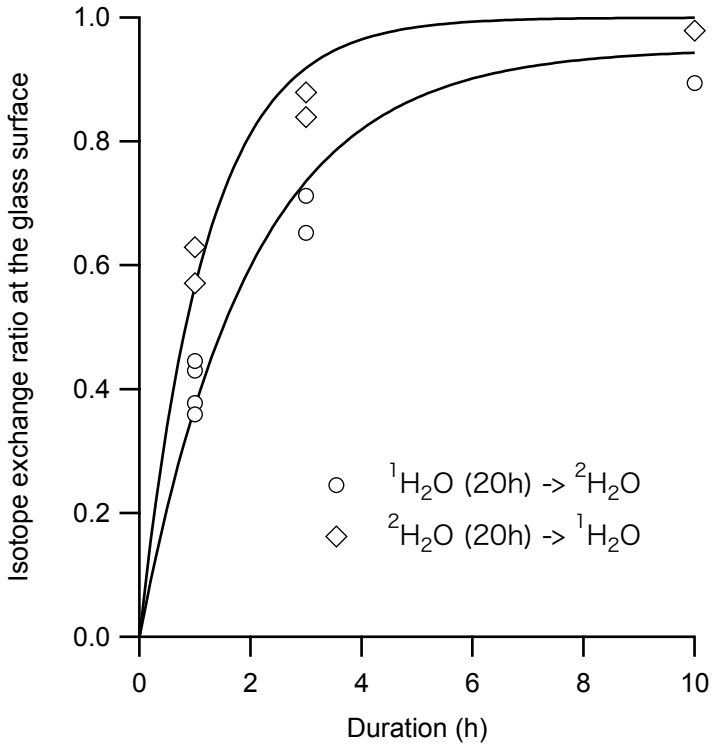

Figure 3-4. The temporal change of hydrogen isotope exchange ratio at the glass surface ($X_{i,\ surface}$) during second-step heating. All data are fitted with Eq. (3-4) (solid curves; see details in the text).

observed in the interior of the glasses.

3-4-2. Diffusion model for hydrogen isotope in silica glass

Hydrogen isotope exchange profiles inside glasses are discussed based on the diffusion model for silica glass (Kuroda et al., 2018) and k_1 and k_2 for the surface reaction. I first assume that there is no difference in diffusivities among ^1H_2O, $^1H^2HO$, and ^2H_2O as observed for diffusion of ^1H_2O and ^2H_2O (Figures 3-1 (a) and (b)). The diffusive change of X_i is expressed as

$$\frac{\partial X_i}{\partial t} = \frac{\partial}{\partial x}\left[D_i \frac{\partial X_i}{\partial x}\right] = \frac{\partial}{\partial x}\left[\left(D_{i_{H_2O}} \frac{\partial X_{i_{H_2O}}}{\partial X_i} + D_{^1H\,^2HO} \frac{\partial X_{^1H\,^2HO}}{\partial X_i}\right)\frac{\partial X_i}{\partial x}\right] \quad (3\text{-}5)$$

where D is the diffusion constant, and x is the diffusion distance. The diffusivity of molecular water ($D_{i_{H_2O}}$ and $D_{^1H\,^2HO}$) has water concentration dependence, and the water diffusivity decreases about 30% along the hydrogen isotope exchange profile (Kuroda et al., 2018). However, D is assumed to be constant in the present study for simplicity because such a decrease of diffusivity does not largely affect the profile fitting and discussion below.

In this case, the diffusion equation can be given as

$$\frac{\partial X_i}{\partial t} = \frac{\partial}{\partial x}\left[D_{molecule} \left(\frac{\partial \left(X_{i_{H_2O}} + X_{{}^1H\,{}^2HO} \right)}{\partial X_i} \right) \frac{\partial X_i}{\partial x} \right] \quad (3\text{-}6)$$

where $D_{molerule}$ represents the diffusivity of molecular water (^1H_2O, $^1H^2HO$, and ^2H_2O). The $\frac{\partial \left(X_{i_{H_2O}} + X_{{}^1H\,{}^2HO} \right)}{\partial X_i}$ term should be represented by the partition coefficient of hydrogen isotope between dissolved molecular water and hydroxyls. Assuming that the partition coefficient is 1 because of high experimental temperature (750°C), the hydrogen isotope exchange reaction inside the glass can be simplified to

$$\frac{\partial X_i}{\partial t} = D_{molecule} \frac{\partial^2 X_i}{\partial x^2}. \quad (3\text{-}7)$$

The diffusion model can explain the isotope exchange profiles of samples (Figure 3-2) and $D_{molecule}$ of 6.6 (±2.0) $\times 10^{-14}$ m^2/s and 8.6 (±1.4) $\times 10^{-14}$ m^2/s were obtained for isotope exchange experiments of ^2H_2O vapor with ^1H in glass and ^1H_2O vapor with ^2H in glass, respectively. The obtained $D_{molecule}$'s are consistent with each other within the error, indicating that the kinetic isotope fractionation for the surface isotope exchange reaction is much larger than that of water diffusion and controls the fractionation observed in this study.

3-4-3. Implications for the mechanisms of hydrogen isotope exchange reaction

I finally discuss the hydrogen isotope exchange mechanism between molecular water and hydroxyls at the glass surface and inside the hydrated glass based on the observation that the surface isotope exchange reaction and water diffusion inside the glass have different effect on kinetic isotope fractionation.

The difference between k_1 and k_2 ($k_1/k_2 = 1.69 \pm 0.21$) might be too large to be explained by the square root of mass ratio of ^1H_2O and ^2H_2O that can be the isotopic fractionation factor related to the reaction involving water molecules. This large difference of k_1 could be explained by a surface reaction mechanism associated with hydrogen atoms, where the kinetic isotopic fractionation factor could $(2/1)^{0.5}$~1.41.

Nolan and Bindeman (2013) performed hydrogen isotope exchange experiments between rhyolite glass and deuterated water at low temperature (20-70°C) and reported that the hydrogen isotope exchange reaction at the glass surface is apparently controlled by proton adsorption and proton exchange with dissolved water in rhyolite glass. If the same mechanism worked at the higher-temperature condition between water vapor and glass surface, the large isotope fractionation at the glass surface could be explained.

More experiments are needed to discuss the effect of hydrogen isotope exchange reaction at the glass surface and inside the glass on kinetic isotope fractionation and to construct the isotope exchange reaction model. However, the present data may indicate that the hydrogen isotope exchange reaction at the glass surface does not reach equilibrium in a few hours, and there could be a large kinetic isotopic fractionation for the surface isotope reaction, which could be the cause of large

hydrogen isotope fractionation during short-time exchange events (e.g., bubble growth in magma).

3-5. Conclusions

Hydrogen isotope exchange experiments between water vapor and hydroxyls in silica glass were performed at 900-750°C and a water vapor pressure of 50 bar. Obtained hydrogen isotope exchange profiles show that the surface isotope exchange reaction and diffusion of hydrogen isotopes, which are carried as molecular water, occur simultaneously. I also found that the surface exchange reaction between $^{1}H_2O$ and ^{2}H in glass proceeds 1.7 times faster than that between $^{2}H_2O$ and ^{1}H in glass, which is a dominant cause of isotope fractionation profiles inside the glasses. The large difference of surface isotope exchange rate implies that a reaction involving hydrogen atoms controls the isotope exchange at the glass surface. The large kinetic isotope fractionation of hydrogen between water vapor and hydroxyls in glass may occur in a time scale of a few hours, and could affect the hydrogen isotope fractionation between dissolved water in magma and bubbles in an ascending magma.

Chapter 4

Fast diffusion path for water in silica glass

4-1. Introduction

Water inside the Earth changes physical and chemical properties of rocks, minerals, and magma. Water circulates into the mantle through subduction zones and back to the surface through arc volcanism. The arc volcanism is affected by water in magma because water changes the physical and chemical properties of magma. For instance, water influences eruption styles through changing magma ascent rates via its influence on bubble nucleation, bubble growth, and degassing (e.g., Sparks, 1978; Rutherford, 2008). Bubble growth in magma is controlled by viscous relaxation and water diffusion, the relative influence of which depends on magma properties such as temperature, pressure, and chemical compositions.

Water diffusion in magma is therefore one of the important basic parameters to control water degassing from magmas. Water diffusion in various silicate glasses, as an analog of silicate melts, has been intensively studied (e.g., Zhang et al., 2007 and references therein). Although the dependences of water diffusion on temperature, water concentration, and pressure have been obtained and formulated, water diffusion in silicate glasses is not yet fully understood as an atomistic-scale process. Kuroda et al. (2018) performed water diffusion experiments in silica glass, and proposed a water diffusion model, where water molecules diffuse through pathways formed by hydroxyls. They also showed that the model is applicable to the water diffusion in various silicate glasses to explain the concentration dependence of water diffusion in rhyolite and basalt glasses.

Here I report a new diffusion pathway of water molecules in silica glass, through which water can be transported at a rate of one-order of magnitude faster than that previously reported values in similar conditions as Kuroda et al. (2018). I discuss the mechanism of water molecule diffusion through the fast pathway and its potential contribution to the water transport in silicate glasses.

4-2. Experimental and analytical methods

Diffusion experiments were performed using the same protocol as in Kuroda et al. (2018). An optical silica glass plate (5 mm × 3 mm × 2 mm; SIGMA KOKI CO.) was flame-sealed in a silica glass tube (3.5 mm and 4.7 mm in inner and outer diameters, and 80 mm in length) with deuterated water (^2H_2O) (7.10-8.17 μL) under atmospheric pressure. The sealed glass tubes were heated in a box furnace at temperatures of 900, 850, 800 and 750 °C for different durations (Table 4-1). The ^2H_2O vapor pressure inside the glass tube was controlled to be 50 bar by complete evaporation of deuterated water.

Polished cross sections of the run products were prepared for measurements of concentration profiles of ^1H, ^2H, and ^{30}Si along the diffusion direction from the glass surface with a secondary ion mass spectrometer (SIMS; Cameca ims-6f) at Hokkaido University. A 15-20 nA Cs+ primary beam was focused to form a 20-25-μm spot on the sample, and

negatively charged secondary ions of ^{1}H, ^{2}H, and ^{30}Si were counted by an electron multiplier for 2, 10, and 1 seconds, respectively, with a 5 μm step. A normal electron flood gun was used for charge compensation. A field aperture was used to permit transmission of ions from the central area of 10 μm in diameter of the sputtered region to minimize the hydrogen signals from absorbed water on the sample surface. A few profiles (mostly three) were obtained for each sample to assess the analytical reproducibility. A starting material glass sample was also measured as a reference with the same analytical condition. The position of the glass surface was determined as being the point from which ^{30}Si counts became constant.

Table 4-1. Experimental conditions and diffusion coefficients of fast water diffusion in silica glass. Errors are 2-sigma standard deviations of the diffusion coefficients evaluated from multiple diffusion profiles. The samples heated for 1 hour and 20 hours were not used to determine the diffusion coefficients because of their short diffusion profiles and homogeneous ^{2}H distributions, respectively.

Run No.	T(°C)	t (hours)	D (m^2/s)
900-1	900	3	1.61 (±0.42) $x10^{-12}$
900-2	900	3	1.87 (±0.60) $x10^{-12}$
900-3	900	20	-
900-4	900	1	-
850-1	850	3	0.92 (±0.25) $x10^{-12}$
850-2	850	3	1.58 (±0.41) $x10^{-12}$
800-1	800	3	0.42 (±0.14) $x10^{-12}$
800-2	800	3	0.66 (±0.11) $x10^{-12}$
800-3	800	3	0.57 (±0.37) $x10^{-12}$
750-1	750	3	0.67 (±0.17) $x10^{-12}$
750-2	750	3	0.55 (±0.08) $x10^{-12}$
750-3	750	20	-

4-3. Results

Diffusion profiles of ^{2}H in samples heated at 900 °C for 1, 3, and 20 hours are compared in Fig. 4-1. The ^{2}H intensity decreases rapidly from rim to core of the sample with diffusion distances of about 50, 100, and 250 μm for the samples heated for 1, 3, and 20 hours, respectively. This is consistent with the diffusion experiments with $^{1}H_2O$ (Kuroda et al., 2018), and the profile shape can be explained by water concentration-dependent diffusion in silica glass (Kuroda et al., 2018), of which detail is discussed below.

It is found that the tail of deuterium profile extends further into the deep region of the sample, where the ^{2}H ion intensity is higher than the original value in the starting material ($^{2}H/^{30}Si < 2 \times 10^{-7}$) (Fig. 4-1). Comparison between the concentration profiles heated at 900°C for 1 and 3 hours clearly shows that ^{2}H migrated into the deeper region of the glass with time (Fig. 4-1). The ^{2}H finally seems to have an almost homogeneous distribution inside the glass after 20-hour heating (Fig. 4-1). This observation clearly shows that a small fraction of deuterium-bearing species migrates at a faster diffusion rate than the dominant fraction that diffuses as the concentration dependent profile. This newly-observed fast diffusion profile was also confirmed in samples heated at 850, 800, and 750 °C (Fig. 4-2).

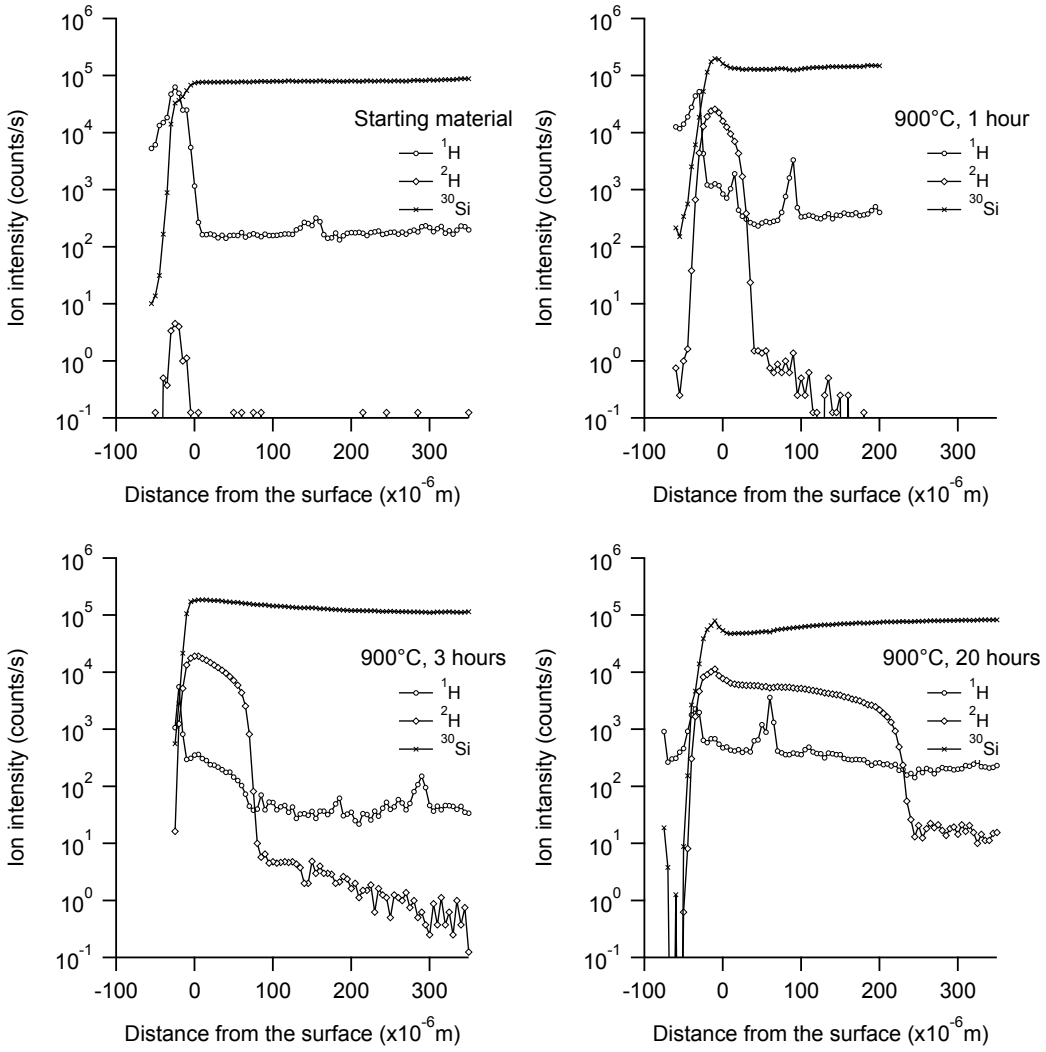

Figure 4-1.

Typical ion intensity profiles of ^{1}H, ^{2}H and ^{30}Si (900 °C for 1, 3, and 20 hours). ^{1}H signals inside the glass are from backgrounds.

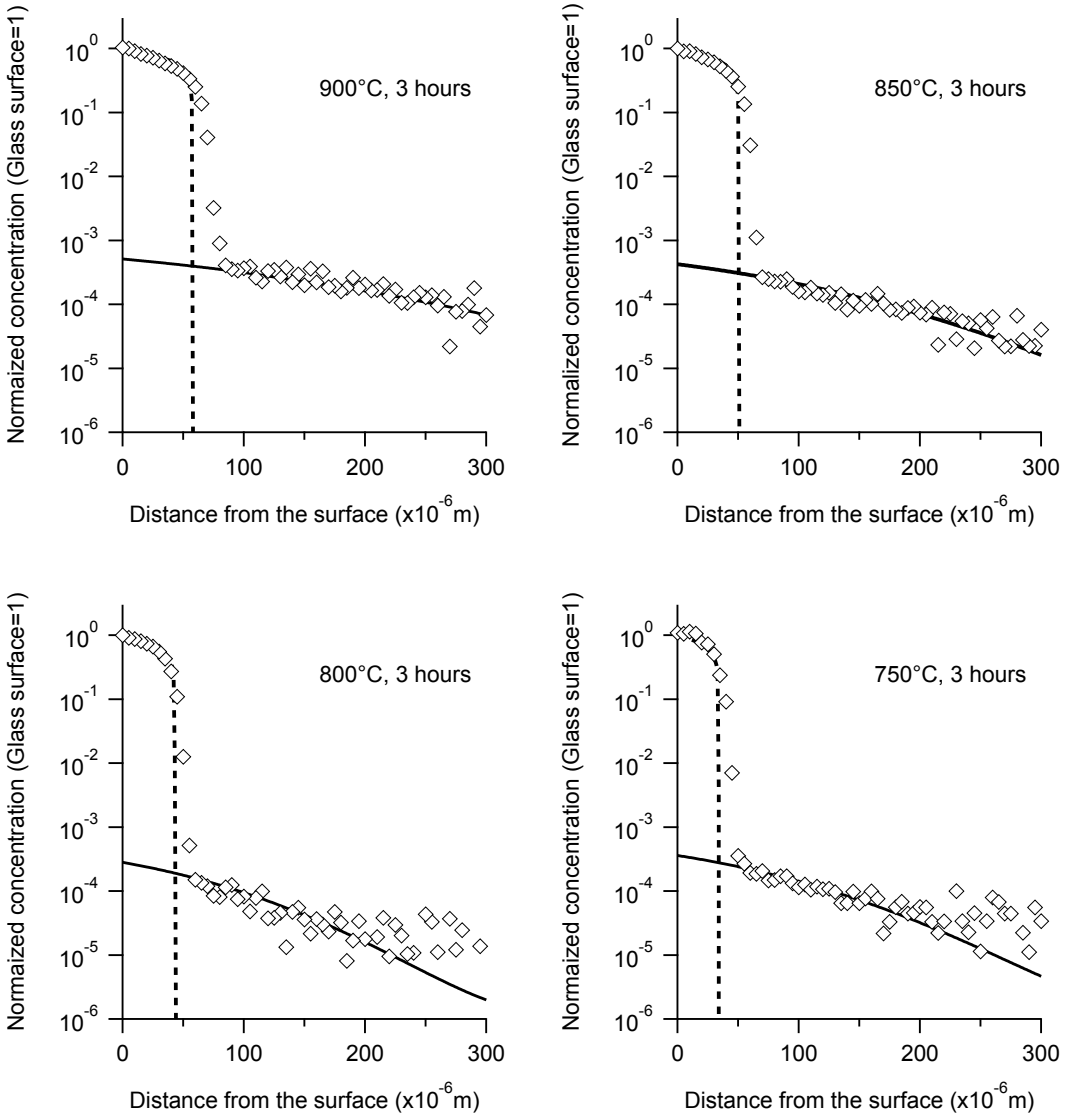

Figure 4-2.

Typical diffusion profiles of ^{2}H, shown as $^{2}H/^{30}Si$ normalized to that at the surface, in silica glass at 900, 850, 800, and 750 °C and a water pressure of 50 bar. The "normal water diffusion"

profiles are fitted with the concentration-dependent water diffusion model (dashed curves) (Kuroda et al., 2018), and the "fast water diffusion" profiles are fitted with the constant-independent water diffusion model (solid curves). All $^{2}H/^{30}Si$ ratios are normalized to the $^{2}H/^{30}Si$ at the glass surface. For fitting of the "normal water diffusion" profiles, D^*, K, and the surface water concentration were taken from Kuroda et al. (2018), where diffusion experiments were performed under the same condition as in the present study (850-650 °C). K and D^* for 900 °C were obtained by the extrapolation of those in Kuroda et al. (2018), and the surface concentration was assumed to be the same as at 850 °C. The surface water concentration of all run products in this study is estimated to be about ~0.3 mol% based on the experiments by Kuroda et al. (2018).

4-4. Discussion

4-4-1. Profile fitting

The profiles of $^{2}H/^{30}Si$ in the run products are used to discuss the $^{2}H_2O$ diffusion because it has a linear relation to the water concentration (Kuroda et al., 2018). The $^{2}H/^{30}Si$ profiles, normalized to the ratio at the glass surface, are shown in Fig. 4-2. The

concentration-dependent diffusion profiles can be explained by the water diffusion model in silica glass (Kuroda et al., 2018), where molecular water is proposed to diffuse through the pathway formed by hydroxyls (-OH). The model attributes the strong water concentration dependence for water diffusion in silica glass to the limited number of diffusion pathways. If water molecules (H_2O_m) favor a pathway formed by cuting Si-O-Si bonds to diffuse in the polymerized silica glass network, water molecules themselves should form the pathways through the hydroxyl formation reaction ($\boldsymbol{H_2O_m + O \leftrightarrow 2OH}$). On the other hand, such pathways preexist in silicate glasses due to the presence of network modifier cations such as Na^+ and K^+ that cut the glass network. This difference results in the stronger water concentration dependence for water diffusion in silica glass than in silicate glasses because the number of diffusion pathways in silica glass depends on water concentration (Kuroda et al., 2018).

The total water diffusivity ($\boldsymbol{D_{H_2O_t}}$) in silica glass through the pathways formed by hydroxyls ('normal diffusion' hereafter) is given by

$$\boldsymbol{D_{H_2O_t} = \frac{D^* K}{8}\left(\left(1 + \frac{16 X_{H_2O_t}}{K}\right)^{\frac{1}{2}} - 1\right)\left(1 - \left(1 + \frac{16 X_{H_2O_t}}{K}\right)^{-\frac{1}{2}}\right)}, \quad (4\text{-}1)$$

where X_i is the molar fraction of species i, D^* is a concentration independent term and K is an equilibrium constant of the hydroxyl formation reaction (Kuroda et al., 2018). The water

diffusion profiles fitted with the diffusion coefficient of Eq. (4-1) are shown as dotted curved in Fig. 4-2. The diffusivities for normal diffusion at the glass surface are about (5-0.8) $\times 10^{-13}$ m^2/s in the present experimental conditions, and decreases with decreasing $\boldsymbol{X_{H_2O_t}}$ in roughly proportion to $\boldsymbol{X^2_{H_2O_t}}$ (Kuroda et al., 2018).

The extended tails of the diffusion profiles ('fast diffusion' hereafter) cannot be explained by the normal diffusion, while they can be fitted by a one-dimensional, semi-infinite diffusion model with a fixed surface concentration and a constant diffusion coefficient (Crank, 1975) assuming that the fast diffusion is independent of the normal diffusion (Fig. 4-2):

$$\boldsymbol{R(x) = (R_s - R_0)\left[1 - erf\left(\frac{x}{2\sqrt{Dt}}\right)\right] + R_0}, \quad (4\text{-}2)$$

where x is the distance from the glass surface, $R(x)$ is the normalized $^2H/^{30}Si$ at x, R_s is the normalized $^2H/^{30}Si$ at the glass surface for fast diffusion, R_0 is the background $^2H/^{30}Si$ relative to R_s, respectively. The fitting curves were obtained for the first ~100-μm of the tails (Fig. 4-2) because the ^2H intensities in the deeper region became comparable to the detection limit. The obtained diffusion coefficients of fast diffusion (Table 4-1) are about one-order of magnitude larger than those of normal water diffusion at the glass surface at all temperatures. They are more than one order of magnitude larger than the normal diffusion coefficients inside the glass

((5-0.8) $\times 10^{-13}$ m^2/s at the glass surface under the present experimental conditions), where the total water concentration is lower than at the surface.

The diffusion model with a constant diffusion coefficient gives R_s of (2–6) $\times 10^{-4}$ at all the temperatures. Although the estimated R_s has a large uncertainty, it is comparable to the homogeneous $R(x)$ within the samples heated for 20 hours ((4–12) $\times 10^{-4}$). This suggests that the assumption of the fixed surface concentration in Eq. (4-2) is valid.

4-4-2. Species and path for fast diffusion of water in silica glass

Mean values of the fast diffusion coefficients at different temperatures, obtained from multiple-line profiles of a single sample, are summarized in Table 4-1. The Arrhenius plot of the fast diffusion coefficient gives an activation energy of 80.5 ± 40.5 kJ/mol and a pre-exponential factor of 6.1 × 10^{-9} m^2/s (Fig. 4-3).

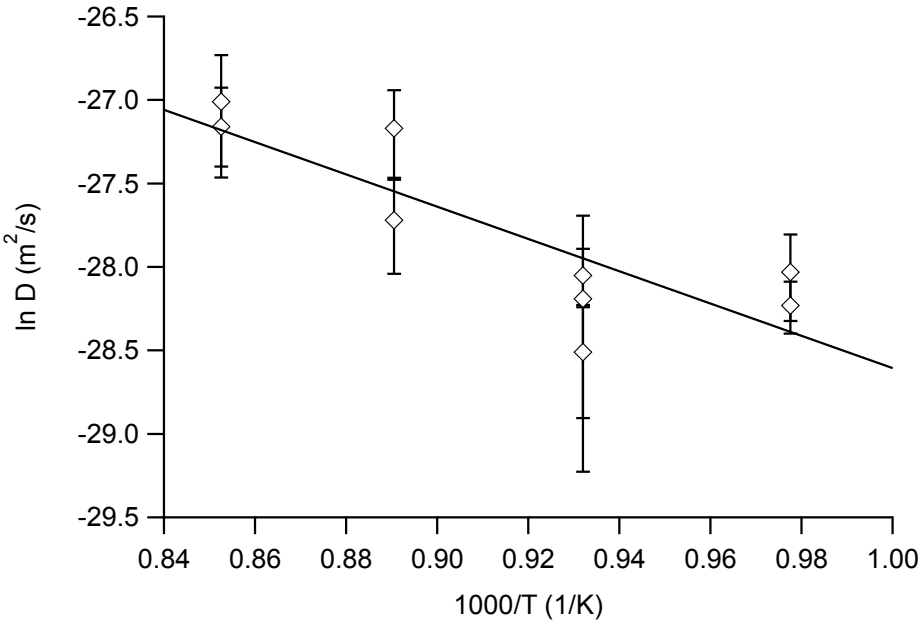

Figure 4-3. The Arrhenius plot of the diffusion coefficient of fast water diffusion (eq. 4-2). The line is a fit to the data. Error bars represent 2-sigma standard deviations of the diffusion coefficients evaluated from multiple diffusion profiles.

The obtained diffusion coefficient at 900-750°C (Table 4-1) is two orders of magnitude smaller than that of H_2 in the same temperature range (Lou et al., 2003), and its activation energy is twice as large as that of H_2 diffusion in silica glass (Lou et al., 2003). Therefore H_2 is unlikely to be a diffusing species for the fast diffusion observed in this study.

The activation energy of ~80.5 kJ/mol is similar to that of the normal diffusion of water in silica glass (e.g., Kuroda et al., 2018; Wakabayashi and Tomozawa, 1989). This indicates that the main diffusion species for fast diffusion is molecular water and that water molecules jump within the glass structure with a similar energetic barrier (Kuroda et al., 2018).

The similar energetic barrier for normal and fast diffusion suggests that the difference in diffusivity should be attributed to factors related to the pre-exponential term for diffusion such as a frequency factor and a diffusion pathway. Here I propose that a small fraction of water molecules diffuse through the pathways connecting free volume (Fig. 4-4) without reacting with the silica glass structure to form hydroxyls. The free volume is the intrinsic gap formed within the polymerized network (e.g., Cohen and Turnbull, 1959; Vrentas and Duda, 1977), and it has been proposed that noble gases diffuse through the free volume in the network structure of silica and silicate glasses (e.g., Behrens, 2010; Amalberti et al., 2016) (Fig. 4-4(a)). In the free-volume diffusion model, the free volumes are connected by "doorways" of an average radius r_0. The activation energy for the diffusion may be given as the energy required to deform the glass network large enough to allow an atom to pass from

one side to another. For instance, the following expression has been proposed for the relationship between the activation energy for diffusion and the atomic radius (r) for noble gases;

$$\boldsymbol{E_a = 8\pi G r_0 (r - r_0)^2}, \quad (4\text{-}3)$$

where G represents a shear modulus of the glass. G and r_0 for silica glass are estimated to be 305 kbar and 1.1 Å, respectively (Anderson and Stuart, 1954).

The obtained diffusivity and the activation energy for the fast diffusion of water molecules are compared with those of noble gas diffusion in silica glass (Swets et al., 1961 for He; Wortmann and Shakelford, 1990 for Ne; Carroll and Stolper, 1991 for Ar; Roselieb et al., 1995 for Kr and Xe) (Fig. 4-4(b)). The radii of noble gasses and molecular water are taken from Zhang and Xu (1995), where molecule radii were obtained by treating the noble gas atoms as ions of zero oxidation states. The free volume diffusion of noble gases in silicate glasses shows the non-Arrhenius relation at temperatures close to the glass transition temperature (e.g., Amalberti et al., 2016) most likely because of the structural change of the glass network. However, the effect of the structural change on the free volume diffusion is negligibly small in this study because the temperature range discussed here is much below the

glass transition temperature of silica glass (~1163°C; Calculated with Deubener et al., 2003), where the free volume diffusion of noble gases show a simple Arrhenius relation.

The activation energies of noble gas diffusion in silica glass show a clear relation with the atomic radius, and they increase with increasing the atomic size (Fig. 4-4(b)). Although the reported activation energies of noble gases are not well fit by the relation with Eq. (4-3), the activation energy for the fast diffusion of molecular water lies on the same trend of noble gas diffusion in silica glass. Moreover, the pre-exponential factor for the fast water diffusion (6.1×10^{-9} m^2/s) fits within the range of those for noble gas diffusion in silica glass (7×10^{-8} and 2×10^{-9} m^2/s for He and Kr, respectively) (Fig. 4-4 (b)). These similarities of activation energy and pre-exponential factors suggest that fast diffusion of molecular water is also governed by molecular jumps between connecting free volume in the silica glass structure.

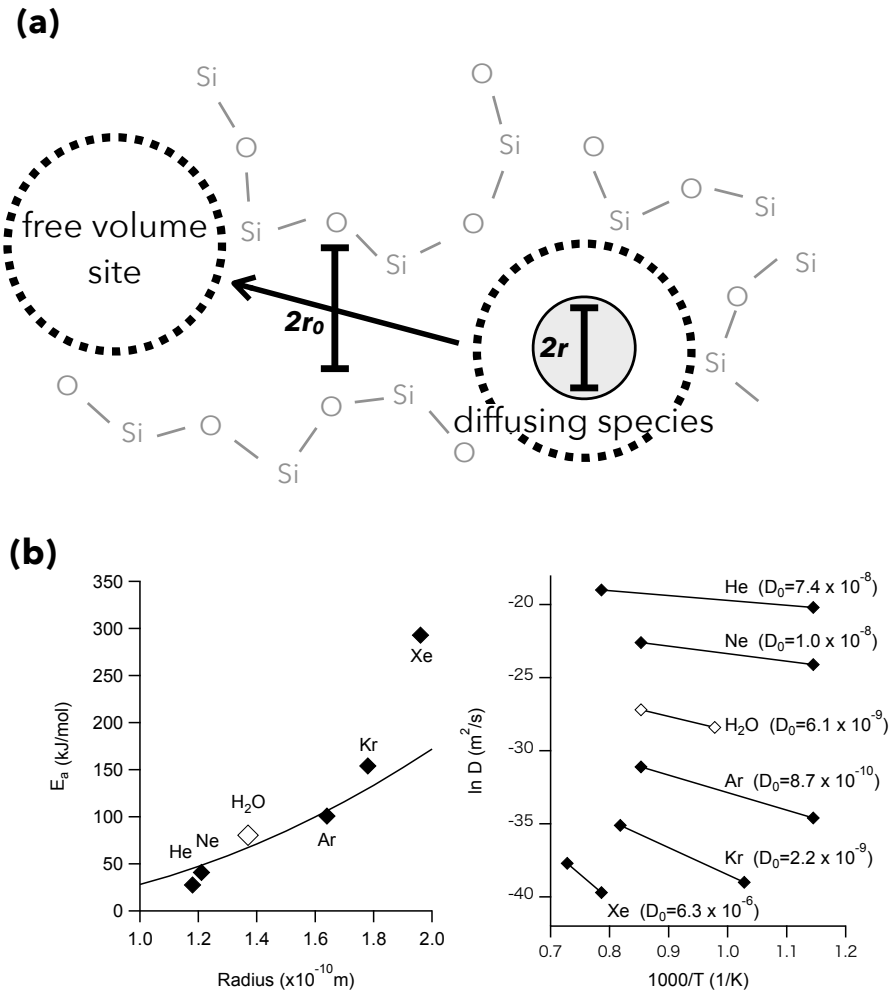

Figure 4-4.

(a) Schematic illustration of the diffusion mechanism through connected free volume. **(b)** Comparisons of activation energy for fast water diffusion and noble gas diffusion in silica glass (left) and of temperature dependence of diffusion coefficients (right). Activation energies

and diffusion coefficients of noble gases in silica glass are taken from Swets et al. (1961) for He, Wortmann and Shakelford (1990) for Ne, Carroll and Stolper (1991) for Ar, and Roselieb et al. (1995) for Kr and Xe. Radii of noble gases and water molecule are taken from Zhang and Xu (1995). The relation between the activation energy and the radius of the diffusing species, obtained with Eq. (4-3) with G = 305 kbar and r_0 = 1.1 Å (Anderson and Stuart, 1954), is also shown.

4-5. Implications

I found that there are, at least, two different pathways for water diffusion in silica glass (normal diffusion through pathways created by the hydroxyl formation reaction and fast diffusion through connected free volume). I here discuss the possible contribution of the fast water diffusion to water transport in silica glass.

The amount of water transported by the fast diffusion can be estimated by integrating the fast diffusion profiles, and it is ~0.5 % of the amount of water transported by normal diffusion at 900 °C. The surface concentration of water for the fast diffusion path is 3-4 orders of magnitude smaller than the total water concentration at the surface (Fig. 4-2). Because the surface concentration of dissolved water under the present experimental conditions is ~0.3 mol% (Kuroda et al., 2018), the surface concentration of fast diffusion is

estimated to range from a few ppm to several hundred ppb. The estimated surface concentration of fast diffusion is likely to represent the water concentration in connected free volume at the surface, and is much smaller than the concentration of free volume in silica glass that was estimated from the solubility of Ar (~0.2 mol%; Shacklford, 1999). This implies that the free volumes were not fully occupied by water molecules at water vapor pressure of 50 bar in the present experiments. I note that water concentration in the starting silica glass is 10 ppm, well below the free volume concentration, such that it should not affect the fast diffusion of ^2H_2O even if the initial water was present in glass' free volumes.

The solubility of molecular water in the fast diffusion path is expected to increase with increasing the water vapor pressure until free volume saturation. The concentration of molecular water occupying the free volume is likely to increase linearly with the water vapor pressure following the Henry's law as noble gases, while the solubility of water in the bulk glass depends on the square root of water vapor pressure (<~200 MPa) (e.g., Zhang et al., 2007).

I emphasize that more experimental work is clearly needed to determine the pressure dependence of water solubility in free volume, but the finding in this study may imply that the contribution of fast water diffusion to water transport in silica glass may become larger under higher water vapor pressures. Especially, its contribution could be significant for water diffusion occurring within a timescale shorter than a few hours as seen in this study, which the

timescale of magma ascent for explosive eruption (e.g., Lloyd et al., 2014). The fast water diffusion might affect the nucleation and growth of bubbles in ascending magma.

4-6. Conclusions

A new fast diffusion path for water was found in the deuterated diffusion experiments in silica glass at 900-750°C and water vapor pressure of 50 bar. The fast diffusion profile was fitted with concentration-independent diffusion model, and the obtained diffusivity is about one order of magnitude larger than that of "water diffusion" reported previously (Kuroda et al., 2018). The obtained activation energy and diffusivity for the fast diffusion indicated that the main diffusion species is molecular water. The fast diffusion coefficient lie on the same trend for noble gas diffusion in silica glass, suggesting that water molecule can diffuse between free volume sites. Contribution of fast diffusion may increase under high water vapor pressure condition, where water molecule diffused into free volume sites may increase. The contribution of fast diffusion could be significant for water diffusion especially occurring within a short timescale, such as nucleation and growth of bubbles in ascending magma.

Chapter 5

General conclusions

In this thesis, I discussed water diffusion in silicate melts and glasses based on diffusion experiments of water in silica glass in order to understand the water diffusion mechanism in silica glass and isotope exchange processes between water vapor and hydroxyls in silica glass and to construct a general water diffusion model in silicate glasses and melts. I focused on the atomistic diffusion mechanism for water in silicate melts and glasses and found that

(1) The water diffusion model for silica glass (Kuroda et al., 2018) is applicable to water diffusion in rhyolite melt taking the effect of water concentration and the activation energy of diffusion into consideration (Chapter 2). The water concentration effect on the activation energy can be attributed to the change of structural dynamical property of melt (i.e., viscosity) due to the increase of non-bridging oxygen atoms in hydrated melts.

(2) A large hydrogen isotope fractionation between water vapor and hydrated glasses may occur in a short timescale (a few to several hours at 750-900°C) because of kinetic isotope fractionation controlled by the surface isotope exchange reaction; $^{1}H_2O$ vapor reacts more rapidly than $^{2}H_2O$ vapor (Chapter 3).

(3) A new diffusion pathway for water molecules is present in silica glass, which connects free volume in the silica glass structure. The water diffusion through the newly found diffusion pathway is one order of magnitude faster than that through the diffusion pathways formed by hydroxyls (Chapter 4).

All the findings in this study suggest that the water behavior in magmas, such as bubble nucleation, bubble growth, and hydrogen isotope fractionation during magma ascent in

an explosive eruption (a few hours to several hours) should be discussed as time-dependent kinetic processes.

There are several issues that should be clarified to apply the results of this study to natural volcanic samples. For instance, all the discussion here is needed to be expanded to a wide range of temperature, pressure, and glass compositions. The reaction model for hydrogen isotope exchange at the glass surface is also required to be refined. More experimental work is required to solve these issues. However, the new observations in the present study shed light on the nature of controlling processes of volcanic eruption style, improving our understanding of the mechanism of water diffusion in silicate melts/glasses, and would make a contribution to better understanding of volcanic activities.

References

Amalberti, J., Burnard, P., Laporte, D., Tissandier, L., and Neuville, D.R. (2016) Multidiffusion mechanisms for noble gases (He, Ne, Ar) in silicate glasses and melts in the transition temperature domain: Implications for glass polymerization. Geochemica et Cosmochemica Acta, 172, 107-126.

Anderson, O.L., and Stuart, D.A. (1954) Calculation of activation energy of ionic conductivity in silica glass by classical methods, Journal of the American Ceramics Society, 37. 573-580.

Anovitz, L.M., Cole, D.R., and Fayer, M. (2008) Mechanisms of rhyolitic glass hydration below the glass transition. American Mineralogist, 93, 1166-1178.

Anovitz, L.M., Cole, D.R., and Riciputi, L.R. (2009) Low-temperature isotope exchange in obsidian: Implications for diffusive mechanisms. Geochemica et Cosmochemica Acta, 73, 3795-3806.

Bansal, N.P., and Doremus, R.H. (1986) Annealing of electron damage in Mid-IR transmitting fluoride glass, Material Research Bulletin, 21, 281-288.

Behrens, H. (2010) Noble gas diffusion in silicate glasses and melts. Reviews in Mineralogy and Geochemistry, 72, 227-267.

Behrens, H., and Zhang, Y. (2001) Ar diffusion in hydrous silicic melts: implications for volatile diffusion mechanisms and fractionation. Earth and Planetary Science Letters, 192, 363-376.

Castro, J.M., Bindeman, I.N., Tuffen, H., and Schipper, C.I. (2014) Explosive origin of silicic lava: Textural and δD-H_2O evidence for pyroclastic degassing during rhyolite effusion. Earth and Planetary Science Letters, 405, 52-61.

Cohen, M.H., and Turnbull, D. (1959) Molecular transport in liquids and glasses. The Journal of Chemical Physics, 31, 1164-1169.

Crank, J. (1975) The Mathematics of Diffusion Second Edition, 414 p. Oxford University Press, Oxford.

Cross, J.K., Roberge, J., and Jerram, D.A. (2012) Constraining the degassing processes of Popocatepetl Volcano, Mexico: A vesicle size distribution and glass geochemistry study, Journal of Volcanology and Geothermal Research, 225-226, 81-95.

Deubener, J., Müller, R., Behrens, H., and Heide, G. (2003) Water and the glass transition temperature of silicate melts. Journal of Non-Crystalline Solids, 330, 268-273.

Doremus, R.H. (1969) The diffusion of water in fused silica, in: J.M. Mitchell et al. (Eds.), Reactivity of Solids, Wiley, New York, p. 667-673.

Doremus, R.H. (1995) Diffusion of water in silica glasses, Journal of Materials Research, 10, 2379-2389.

Doremus, R.H. (1999) Diffusion of water in crystalline and glassy oxides: Diffusion-reaction model. Journal of Materials Research, 14, 3754-3578.

Doremus, R.H. (2000) Diffusion of water in rhyolite glass: diffusion-reaction model,

Journal of Non-Crystalline Solids, 261, 101-107.

Eyring, H. (1936) Viscosity, plasticity, and diffusion as examples of absolute reaction rates, Journal of Chemical Physics, 4 (1936) 283-291.

Falenty K., and Webb, S.L. (2010) Shear modulus, heat capacity, viscosity and structural relaxation time of Na_2O-Al_2O_3-SiO_2 and Na_2O-Fe_2O_3-SiO_2 melts, Physics and Chemistry of Minerals, 37, 613-634.

Fulcher, S. (1925) Analysis of recent measurements of the viscosity of glasses, Journal of the American Ceramics Socsiety, 8, 339-355.

Deubener, J., Muller, R., Behrens, H., Heide, G. (2003) Water and the glass transition temperature of silicate melts, Journal of Non-Crystalline Solids, 330, 268-273.

Hess, K.U., and Dingwell, D.N. (1996) Viscosity of hydrous leucogranitic melts: a non-Arrhinian model, American Mineralogist, 81, 1297-1300.

Kuroda, M., Tachibana, S., Sakamoto, N., Okumura, S., Nakamura, M., and Yurimoto, H. (2018) Water diffusion in silca glass through pathways formed by hydroxyls, American Mineralogist, 103, 412-417.

Kuroda, M., Tachibana, S., Sakamoto, N., and Yurimoto, H. (2019) Fast diffusion path for water in silica glass, American Mineralogist, 104, in press.

Kyser, T.K, and O'Neil, J.R. (1984) Hydrogen isotope systematics of submarine basalts. Geochemica et Cosmochemica Acta, 48, 2123-2133.

Lapham, K.E., Holloway, J.R., and Delaney, J.R. (1984) Diffusion of H_2O and D_2O in obsidian at elevated temperatures and pressures. Journal of Non-Crystalline Solids, 67, 179-191.

Liu, Y., Anderson, A.T., and Wilson, C.J.N. (2007) Melt pockets in phenocrysts and decompression rates of silicic magmas before fragmentation. Journal of Geophysical Research, 112, B06204.

Losq C.L., Moretti, R., and Neuville, D.R. (2013) Speciation and amphoteric behavior of water in aluminosilicate melts and glasses: high-temperature Raman spectroscopy and reaction equilibria, European Journal of Mineralogy, 25, 777-790.

Lloyd, A.S., Euprecht, P., Hauri, E.H., Rose, W., Gonnermann, H.M., and Plank, T. (2014) NanoSIMS results from olivine-hosted melt embayments: Magma ascent rete during explosive basaltic eruptions, Journal of Volcanology and Geothermal Research, 283, 1-18.

Lou, V., Sato, R., and Tomozawa. M. (2003) Hydrogen diffusion in fused silica at high temperatures, Journal of Non-Crystalline Solids, 315, 13-19.

Martel, C., and Iacono-Marziano, G. (2015) Timescales of bubble coalescence, outgassing, and foam collapse in decompressed rhyolitic melts, Earth and Planetary Science Letters, 412, 173-185.

Massol, H., and Koyaguchi, T. (2005) The effect of magma flow on nucleation of gas bubble in a volcanic conduit. Journal of Volcanology and Geothermal Research, 143, 69-88.

Mcintosh, I.M., Nichols, A.R.L., Tani, K., and Llewelln, E.W. (2017) Accounting for the species-dependence of the 3500 cm^{-1} H_2O_t infrared molar absorptivity

coefficient: Implications for hydrated volcanic glasses. American Mineralogist, 102, 1677-1689.

Nakamura, M., Kasai, Y., Sato, N., and Yoshimura, S. (2008) Application of hydrogen isotope geochemistry to volcanology: Recent perspective on eruption dynamics. AIP Conference proceedings, 987, 93.

Ni, H., Xu, Z., and Zhang, Y. (2013) Hydroxyl and molecular H_2O diffusivity in a haploandesitic melt. Geochemica et Cosmochemica Acta, 103, 36-48.

Ni, H., Hui, H., and Neumann, G.S. (2015) Transport properties of silicate melts, Reviews of Geophysics, 53, 715-744.

Nolan, G.S., and Bindeman, I.N. (2013) Experimental investigation of rates and mechanisms of isotope exchange (O, H) between volcanic ash and isotopically-labeled water. Geochemica et Cosmochemica Acta, 111, 5-27.

Nowak, M., and Behrens, H. (1997) An experimental investigation of diffusion of water in haplogranitic melts, Contribution of Mineralogy to Petrology, 126, 365-376.

Oeser, M., Dohmen, R., Horn, I., Schuth, S., and Weyer, S. (2015) Processes and time scales of magmatic evolution as revealed by Fe-Mg chemical and isotopic zoning in natural olivines, Geochemica et Cosmochemica Acta, 154, 130-150.

Persikov, E.S., Newman, S., Bukhitiyarov, P.G., Nekrasov, A.N., and Stolper, E.M. (2010) Experimental study of water diffusion in haplobasaltic and haploandesitic melts, Chemical Geology, 276, 241-256.

Persikov, E.S., Bukhiyarov, P.G., Nekrasov, A.N., and Bondarenko, G.V. (2014) Concentration dependence of water diffusion in obsidian and dacitic melts at

high-pressures, Geochemical International, 52, 365-371.

Roselieb, K., Rammensee, W., Büttner, H., and Rosenhaure, M. (1995) Diffusion of noble gases in melts of the system SiO_2-$NaAlSi_2O_6$. Chemical Geology, 120, 1-13.

Rutherford, M.J. (2008) Magma Ascent Rates, Reviews in Mineralogy and Geochemistry, 69, 241-271.

Schilling, F.R., and Sinogeikin, S.V. (2003) Elastic properties of model basaltic melt compositions at high temperatures, Journal of Geophysical Research, 108, B6.

Shackelford, J.F. (1999) Gas solubility in glasses – principles and structural implications. Journal of Non-Crystalline Solids, 231-241.

Sio, C.K.I., Dauphas, N., Teng, F.Z., Chaussidon, M., Helz, R.T., and Roskosz, M. (2013) Discerning crystal growth from diffusion profiles in zoned olivine by *in situ* Mg-Fe isotopic analyses, Geochemica et Cosmochemica Acta, 123, 302-321.

Sparks, R.S.J. (1978) The dynamics of bubble formation and growth in magmas: a review and analysis, Journal of Volcanology and Geothermal Research, 3, 1-37.

Stolper, E. (1982) Water in silicate glasses: An infrared spectroscopy study. Contributions to Mineralogy and Petrology, 81, 1-17.

Swets, D.E., Lee, R.W., and Frank, R.C. (1961) Diffusion coefficients of helium in fused quarts, The Journal of Chemical Physics, 34, 17-22.

Takahashi, E. (1980) Thermal history of lherzolite xenoliths-I. Petrology of lherzolite xenoliths from the Ichinomegata crater, Oga peninsula, northeast Japan, Geochemica et Cosmochemica Acta, 44, 1643-1658.

Taylor, B.E., Eichelberger, J.C., and Westrich, H.R. (1983) Hydrogen isotopic evidence of rhyolitic magma degassing during shallow intrusion and eruption. Nature, 306, 8, 541-545.

Tomozawa, M., Li, H., and Davis, K.M. (1994) Water diffusion, oxygen vacancy annihilation and structural relaxation in silica glasses, Journal of Non-Crystalline Solids, 179, 162-169.

Toramaru, A. (1989) Vesiculation process and bubble size distribution in ascending magmas with constant velocities, Journal of Geophysical Research, 94, 17,523-17,542.

Vrentas, J.S., and Duda, J.L. (1977) Diffusion in polymer – solvent systems. i. reexamination of the free-volume theory. Journal of Polymer Sciene, 15, 403-416.

Wakabayashi, H., and Tomozawa, M. (1989) Diffusion of water into silica glass at low temperature. Journal of the American Ceramic Society, 72, 1850-1855.

Wortman, R.S., and Shackelford, J.F. (1990) Gas transport in vitreous silica fibers. Journal of Non-Crystalline Solids, 125, 280-286.

Zhang, L., Guo, X., Wang, Q., Ding, J., and Ni, H. (2017) Diffusion of hydrous species

in model basaltic melt. Geochemica et Cosmochemica Acta, 215, 377-386.

Zhang, Y. (1999) H_2O in rhyolitic glasses and melts: Measurement, speciation, solubility, and diffusion. Reviews of Geophysics, 37, 493-516.

Zhang, Y., Stolper, E.M., and Wasserburg, G.J. (1991) Diffusion of water in rhyolitic glasses. Geochemica et Cosmochemica Acta, 55, 441-456.

Zhang, Y., and Xu, Z. (1995) Atomic radii of noble gas elements in condensed phases, American Mineralogist, 80, 670-675.

Zhang, Y., and Behrens, H. (2000) H_2O diffusion in rhyolitic melts and glasses, Chemical Geology, 169, 243-262.

Zhang, Y., Xu, Z., and Liu, Y. (2003) Viscosity of hydrous rhyolitic melts inferred from kinetic experiments, and a new viscosity model, American Mineralogy, 88, 1741-1752.

Zhang, Y., Xu, Z., Zhu, M., and Wang, H. (2007) Silicate melt properties and volcanic eruptions, Reviews of Geophysics, 45, RG 4004.

Zhang, Y., and Ni, H. (2010) Diffusion of H, C, and O components in silicate melts, Reviews of Mineralogy and Geochemistry, 72, 171-225.

Acknowledgments

I am indebted to my supervisors, Professor Shogo Tachibana (U. of Tokyo) and Professor Hisayoshi Yurimoto (Hokkaido Univ.). They always gave me the opportunities to make my study as my desires and gave me lots of support to do what I want. I also had numerous valuable discussions with them through this work, which are really interesting for me. I am happy that I could study in their lab and enjoyed my research for a long period of six years.

I also thank other members of my doctoral committee, Professor Takaya Nagai, and Dr. Junji Yamamoto for their advice and valuable comments.

I am deeply grateful to Dr. Naoya Sakamoto (Hokkaido Univ.) and Dr. Isao Sakaguchi (NIMS) for their skillful help with SIMS measurements and numerous encouragements. They always gave me suggestions in finding research themes, performing experiments and SIMS measurements since I had been an undergraduate student. Without their help, this paper would not have materialized.

I am also thanking Dr. Ryosuke Fujita (Kyusyu Univ.), Dr. Koji Takahashi (AIST), and Dr. Ayumi Okamoto for their kindly advice and encouragements when I bogged down. They always care about me and listened to my story even after they leave Hokkaido University.

Furthermore, I am grateful to other staffs, students and former members of Tachibana Lab and Yurimoto Lab for many helpful suggestions and encouragements. I would like to thank all of those who spent a hard but fun working time with me.